D E S I G N O F A L A R G E
W A T E R T U N N E L

Thesis by

Thomas V Davis

In Partial Fulfillment of the Requirements

For the Degree of

Aeronautical Engineer

California Institute of Technology

Pasadena, California

1948

ACKNOWLEDGEMENT

The author wishes to thank Professor E.E. Sechler for his fine guidance and for his patient discussion of many of the points involved in the analysis.

ABSTRACT

A ten-foot-diameter water tunnel is discussed as to feasibility and design, and consideration is narrowed to the working section -- nozzle, throat and diffuser. A non-cavitating nozzle shape is calculated by systematizing the method suggested by Hsue-Shen Tsien.

Structural design is approached on the basis of a six-hundred-foot static pressure head; and an additional half-full design loading is calculated as a Fourier expansion. The analysis of the structure is broken down into a number of elasticity problems.

The cylindrical throat is analyzed by membrane theory for the high-head condition; and stresses at and in the supporting rings are thoroughly investigated. More involved methods considering transverse shear and bending are used to check the stability of the shell when only partially full.

Membrane theory is applied to the conical diffuser and to the double-curved nozzle to determine the stress state in both under the high-head condition. Shell thicknesses and member sizes have been selected throughout from this analysis.

TABLE OF CONTENTS

DESIGN OF A LARGE WATER TUNNEL

I. INTRODUCTION

Background:

Present trends in water tunnel design are toward both larger sizes and greater speeds, so it seems worth speculating on what might be done if one were to utilize the power available at one of our large western damsites. Actually, it is not the purpose of this paper to establish the feasibility of such a plan. Rather, it is hoped to establish some of the more complicated analysis procedures which one might expect to encounter in the design of such a structure.

Supposing the tunnel to operate as a penstock on the reservoir water and head for purposes of simplification, dam height would limit the velocity attainable. Within the limit of total head obtainable, variations of velocity and pressure head might be obtained by installing needle valves both upstream and downstream of the working section. The upstream valves would have to be at the beginning of a long straight run of penstock to minimize turbulence at the working-section end.

Problem:

The structural considerations in a tunnel of any size are many and complex; and this report can be only a small part of the complete analysis which one would have to undertake before detail design could be begun. Therefore, the following is limited to the working venturi section -- nozzle, throat and diffuser. Primarily, the problem is one of thin-sheet analysis by the methods of theory of elasticity; but other interesting problems appeared in the study.

When the nozzle shape was under consideration, no particularly neat system for carrying out the calculations developed by Hsue-Shen Tsien in his paper "On the Design of the Contraction Cone for a Wind Tunnel"[1] could be found; so a series of tables were developed to make repetition of the process as simple as possible. Also, derivatives of the probability curve up to the twenty-third were calculated and these can be used in future calculations directly. The calculations for a 13:10 reduction in diameter have been included as relevant and at the same time useful examples.

At one point a useful Fourier expansion was indicated; and these results are included. The calculations have been systematized so that increased accuracy can be obtained if desired by extending the series. Further, this particular expansion will be invaluable when the half-full design condition is applied to the conical and double-curved portions of the tunnel.

Breakdown:

The second section is devoted to developing the physical layout as it might be expected to be built. This is mostly descriptive; but the Tsien analysis is included at this point. That is, the basic equations and conclusions are presented; but the actual calculations are given by tables in Appendix A.

In the third section, design conditions are established with regard to expected loads. One of the design conditions is the probable maximum static pressure head plus a factor for the impact of closing the downstream needle valves. This condition retains the cylindrical shape by high pressures all around the circumference. The part-full condition is the other; and under this condition, the cylinder must maintain its shape by its own stiffness. Since the solution of the stress state involves infinite series solutions, the part-full loading condition has been expressed as a Fourier series; and the result is given in the third section with actual calculations relegated to Appendix B.

Dynamic effects have not been considered here although they could be obtained from the fluid flow equations and would be particularly important for anchorage. The conical and double-curved portions of the tunnel should be investigated for dynamic effects.

The fourth section contains the actual thin-sheet analysis of the cylindrical portion of the tunnel. The high-head loading condition is used to determine the overall stress state by

membrane theory and to analyze the local conditions at supporting rings by methods which consider bending stresses in the sheet. The part-full loading condition is used to obtain an overall stress state involving bending moments in the sheet for purposes of checking buckling possibilities. Local stresses at the supporting rings are relatively unimportant under the low-head loading condition.

The fifth and sixth sections contain discussions of the conical and double-curved portions of the tunnel respectively; and are particularly concerned with application of the techniques of section four to problems of increasing degrees of difficulty. The high-head membrane-theory approach has been applied to the conical diffuser and to the nozzle; but time did not permit of the more involved and tedious analyses of the part-full analysis.

In the seventh section, some conclusions are presented as to the usefulness and accuracy of the analysis contained herein. This is followed by the Appendix which contains calculations relative to the Tsien and Fourier analyses.

II. PHYSICAL LAYOUT

General Plan for Working Section:

The plan as presented here is no less than grandiose; but the problems are about the same regardless of any scale change of several times up or down. The illustration on the next sheet gives an idea of the magnitude of the project as herein proposed. Obviously there are many very interesting problems in such a design; but only the thin-sheet analysis is possible in this paper.

The flow enters from a thirteen-foot diameter penstock at the left of the illustration. The penstock should be straight for as far as possible back toward the dam and the upstream control needle valves. At (C), the flow is contracted in an eighteen-foot-long nozzle of special design to smooth out the flow and to speed it up. Ring stiffeners and supports at either end of the nozzle are seated on concrete bases designed to take the thrust of dynamic effects. It is almost certain that additional stiffeners will be necessary to transfer axial loads from the nozzle shell to the concentration points of support.

Straight cylindrical portions of ten-foot diameter form the throat of this giant venturi. Approximately six-foot lengths are cantilevered from the smaller ends of both nozzle and diffuser with flanges for bolting to the main working section which is removable. It is considered more interesting

Davis_tv-1948
p. 6

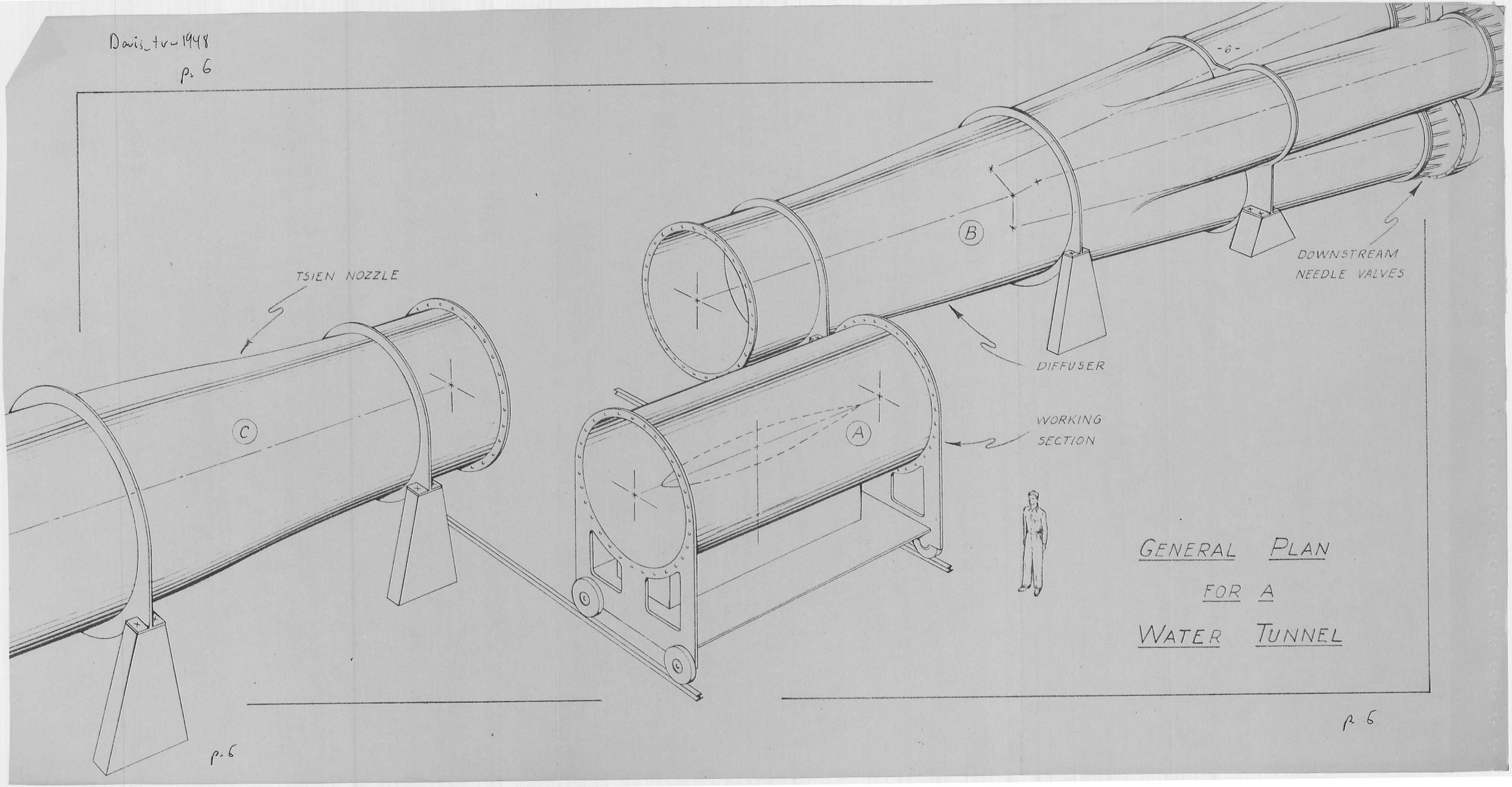

GENERAL PLAN FOR A WATER TUNNEL

p. 6

p. 6

for purposes of this paper to assume a removable portion (A) which can be analyzed as a continuous cylindrical shell. In the illustration of page 6, an eighteen-foot length has been shown as mounted on a car which runs in and out on two rails. Access doors would be more practical, but it is desired to develop the complete cylinder analysis as preparatory to the conical and double-curved analyses.

The diffuser section (B) is conical with elements inclined at approximately five degrees to the axis and forms an eighteen-foot-long frustrum. Stiffening rings similar to those for the nozzle support the diffuser on similar concrete bases. The next eighteen-foot section approximates three seven-and-one-half-foot diameter pipes with their axes inclined at five degrees to the main tunnel axis. Actually, this is a transition leading into individual pipes which after another eighteen feet flange for attachment to the three downstream needle valves for control of back-pressure or simulated running-depth.

Altogether, this description of a general plan is intended only to bring out certain problems which might be encountered in the analysis of such a structure. Therefore, theoretical investigations of the type undertaken herein are advantageous at this time for the analysis techniques which they establish for ultimate application to any final design which might be conceived. The procedure so carefully established for the cylindrical portion of the tunnel is equally

applicable to the penstock or to any large pipeline.

(blank)

Tsien Analysis of Nozzle Section:

One of the first problems of physical layout that arose was that of a suitable length and shape of the contracting nozzle which leads into the tunnel throat. Since double-curved surfaces are involved which will likely necessitate machining whether curved sheet or casting is employed, the

shortest possible nozzle is to be desired. However, contracted flows are accelerated flows and the attendant pressure drop is fraught with cavitation dangers. This problem was attacked by Hsue-Shen Tsien in his paper "On the Design of the Contraction Cone for a Wind Tunnel" which was published in the February, 1943, issue of the Journal of the Aeronautical Sciences (vol. 10, no. 2, p. 68). No attempt will be made to repeat his derivation here; but a recitation of steps in the procedure will aid anyone desiring to repeat the process for some other contraction ratio.

In this design, a contraction ratio of diameters had been established at 13:10 and the resulting velocity ratios must needs be 0.592:1. Dr. Tsien assumes that flow along the axis of the nozzle can be expressed in the following form:

$$u_o(x) = 0.796 + 0.408 \int_0^x \frac{1}{\sqrt{2\pi}} e^{-\frac{x^2}{2}} dx \qquad \text{and}$$

$$v_o(x) = 0 \qquad \text{by symmetry.}$$

Consistent with this assumption are the ones of initial and final velocity:

$$u(-\infty, r) = 0.592$$
$$u(\infty, r) = 1.00, \qquad \text{and}$$
$$v(\pm\infty, r) = 0$$

These are boundary conditions on the two fundamental equations of hydrodynamics:

$$\frac{\partial v}{\partial x} + \frac{\partial u}{\partial r} = 0 \qquad \text{(irrotational condition)}$$

$$\frac{\partial}{\partial x}(ru) + \frac{\partial}{\partial r}(rv) = 0 \qquad \text{(continuity equation)}$$

The boundary condition assumed along the axis is the trick that makes the Tsien solution so very neat.

Note that the integral in the assumed velocity distribution along the x-axis is exactly the area under the probability curve:

$$\Phi(x) = \frac{1}{\sqrt{2\pi}} e^{-\frac{x^2}{2}}$$

which function is tabulated in many mathematical tables together with its first few derivatives. Further, the derivatives of this function have the following recurrence relation:

$$\Phi^{(m)}(x) = -\left[x\,\Phi^{(m-1)}(x) + (m-1)\,\Phi^{(m-2)}(x)\right].$$

These functions have been calculated and tabulated in Appendix A up to the nineteenth derivative; and the table can be extended readily if greater accuracy is desired in subsequent calculations. These values are applicable to any future solution for a different contraction ratio.

The solution determined by Tsien takes the form:

$$u(x,r) = u_o(x) + 0.408 \sum_{n=1}^{\infty} \frac{(-1)^n}{(n!)^2}\left(\frac{r}{2}\right)^{2n} \Phi^{(2n-1)}(x)$$

$$v(x,r) = 0.408 \sum_{n=1}^{\infty} \frac{(-1)^n n}{(n!)^2}\left(\frac{r}{2}\right)^{2n-1} \Phi^{(2n-2)}(x)$$

$$= -0.408\, r \sum_{n=0}^{\infty} \frac{(-1)^n}{(n+1)(n!)^2}\left(\frac{r}{2}\right)^{2n} \Phi^{(2n)}(x).$$

The actual streamlines are determined by calculating a grid of values of the stream function:

$$\Psi(x,r) = \int_0^r r \cdot u(x,r) \cdot dr \qquad \text{or}$$

$$= 0.398 r^2 + 0.204 r^2 \int_0^x \Phi(x) \cdot dr +$$

$$0.204 r^2 \sum_{n=1}^{\infty} \frac{(-1)^n}{(n+1)(n!)^2} \left(\frac{r}{2}\right)^{2n} \Phi^{(2n-1)}(x).$$

The actual calculation of these functions is to be found in Appendix A; and the results are plotted on the next sheet. The following sheet shows the contour for $\Psi = 0.6$ expanded to the required scale; and the resultant velocities along axis and wall have been plotted on the basis of tunnel velocity equal to one. The resultant velocity at any point in the flow is readily calculated from:

$$w(x,r) = \sqrt{u^2(x,r) + v^2(x,r)}.$$

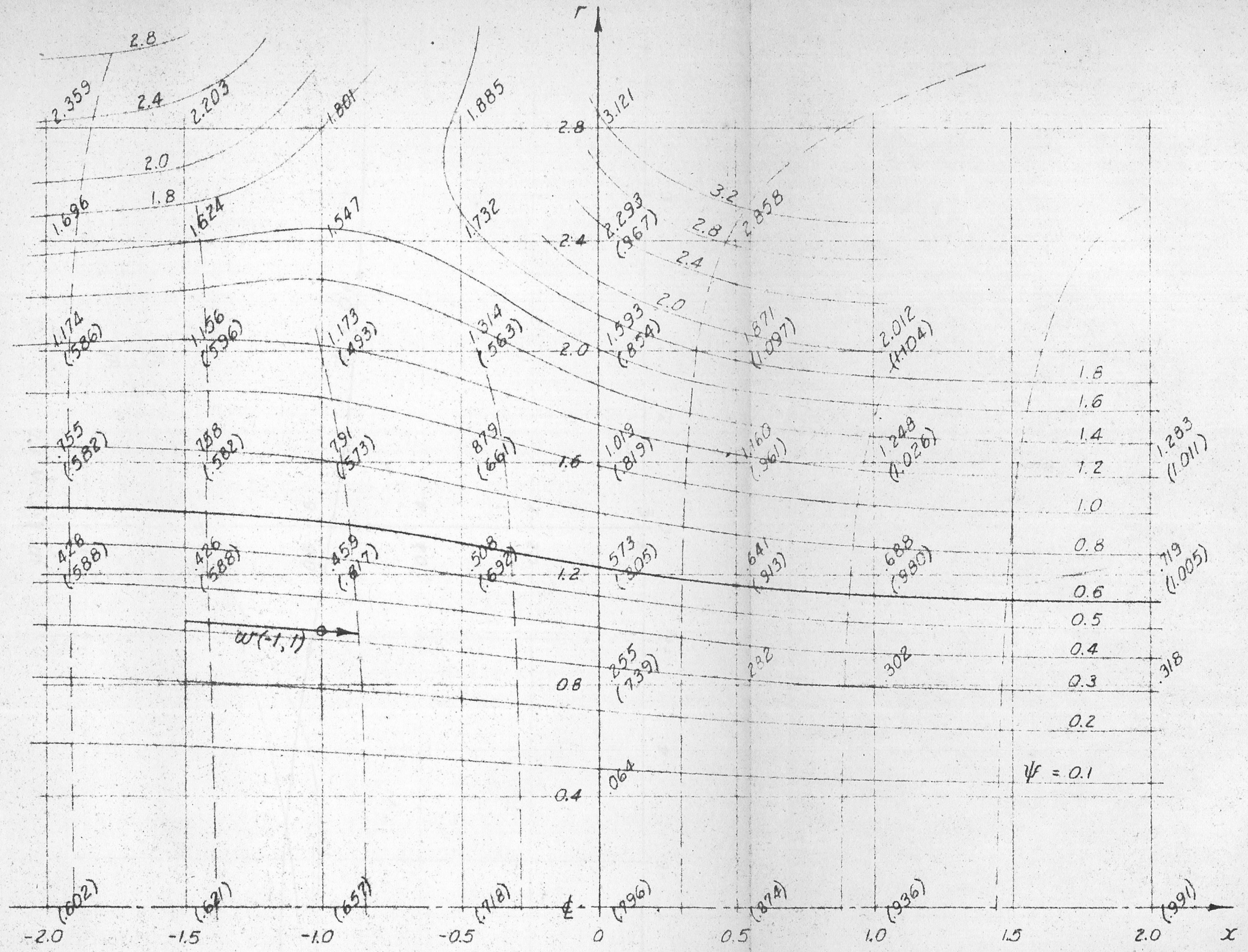

NOZZLE STREAMLINES

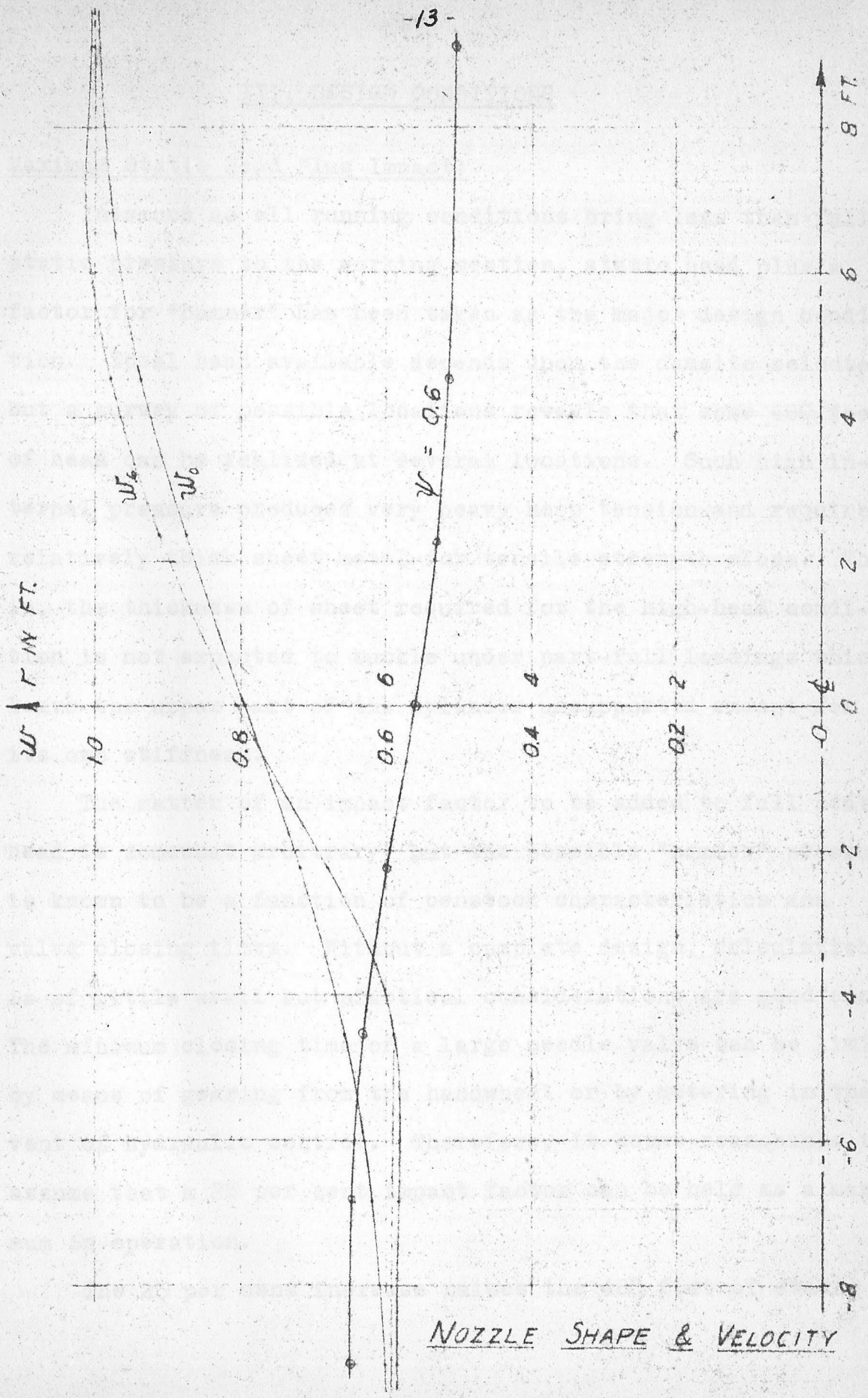

NOZZLE SHAPE & VELOCITY

III. DESIGN CONDITIONS

Maximum Static Head Plus Impact:

Inasmuch as all running conditions bring less than full static pressure to the working section, static head plus a factor for "hammer" has been taken as the major design condition. Total head available depends upon the damsite selected; but a survey of possible locations reveals that some 480 feet of head can be realized at several locations. Such high internal pressure produces very heavy hoop tension and requires relatively thick sheet metal for tensile strength alone. That is, the thickness of sheet required for the high-head condition is not expected to buckle under part-full loadings which leave the upper part of the cylinder unsupported except for its own stiffness.

The matter of an impact factor to be added to full static head is somewhat arbitrary; but the possible "hammer" pressure is known to be a function of penstock characteristics and valve closing times. Without a complete design, calculation is of little avail but practical considerations are good enough. The minimum closing time of a large needle valve can be limited by means of gearing from the handwheel or by metering in the event of hydraulic control. Therefore, it seems reasonable to assume that a 25 per cent impact factor can be held as a maximum in operation.

The 25 per cent increase raises the 480 feet of static

head to 600 feet of design pressure head. This corresponds to a design pressure of 37.5 kips per square foot or 260 pounds per square inch.

Part-Full Condition:

During the process of filling or emptying the penstock, the tunnel section will be under the full range of heads from -5 feet to 480 feet over the center-line datum. The problem here is to investigate the most critical loading condition. The high-head condition already discussed produces maximum hoop tension but transverse bending moments are insignificant except near the supporting rings. Under heads less than +5 feet, with not all of the sheet supported by internal pressure, transverse bending stiffness becomes important over-all and the possibility of buckling must be investigated.

It so happens that the critical hydrostatic loading has been established. Roark,[2] in his chapter on beams, solves the problem of an elemental length of circular cylinder supported by shears distributed sinusoidally around its circumference and loaded by the radial pressures of a liquid only partially filling the cylinder (case 27 of chapter 8). This is exactly the condition of the elements of the working section which might buckle; and the maximum transverse bending moment is seen to result from having the cylinder half-full.

The half-full pressure distribution is a function of the angular position of the point being considered. That is, there

is zero pressure over the upper half of the cylinder; and the pressure over the lower half is directly proportional to the -cosine ϕ (see next sheet). As can be seen in the plot given, the first derivative of the pressure function is discontinuous at the two ends of the horizontal diameter -- "and there's the rub."

Two procedures of about equal difficulty in their application suggest themselves at this point. The more usual and seemingly the more direct approach would be to treat the upper and lower halves of the cylinder as two separate problems. For a complete answer, this method involves fitting the boundary conditions of the two problems along the two elements they have in common. The techniques are well established and the major part of the work involved in solving the deflection pattern lies in fitting these boundary conditions. Further, the problem becomes more difficult and must be repeated for the conical and the double-curved sections. Another approach circumvents the work of fitting intermediate boundary conditions and will do much to lessen the labor of analyzing the more complicated surfaces.

The fact that plate deflection problems are generally approached by assuming doubly-infinite Fourier series for the solution suggests a Fourier series expansion for the half-full pressure distribution. This representation avoids the discontinuities and fits into the form of the solution to be under-

n	b_n
0	$\frac{1}{\pi}$
1	$-\frac{1}{2}$
2	$\frac{2}{3\pi}$
4	$-\frac{2}{15\pi}$
6	$\frac{2}{35\pi}$
8	$-\frac{2}{63\pi}$
10	$\frac{2}{99\pi}$
12	$-\frac{2}{143\pi}$
14	$\frac{2}{195\pi}$

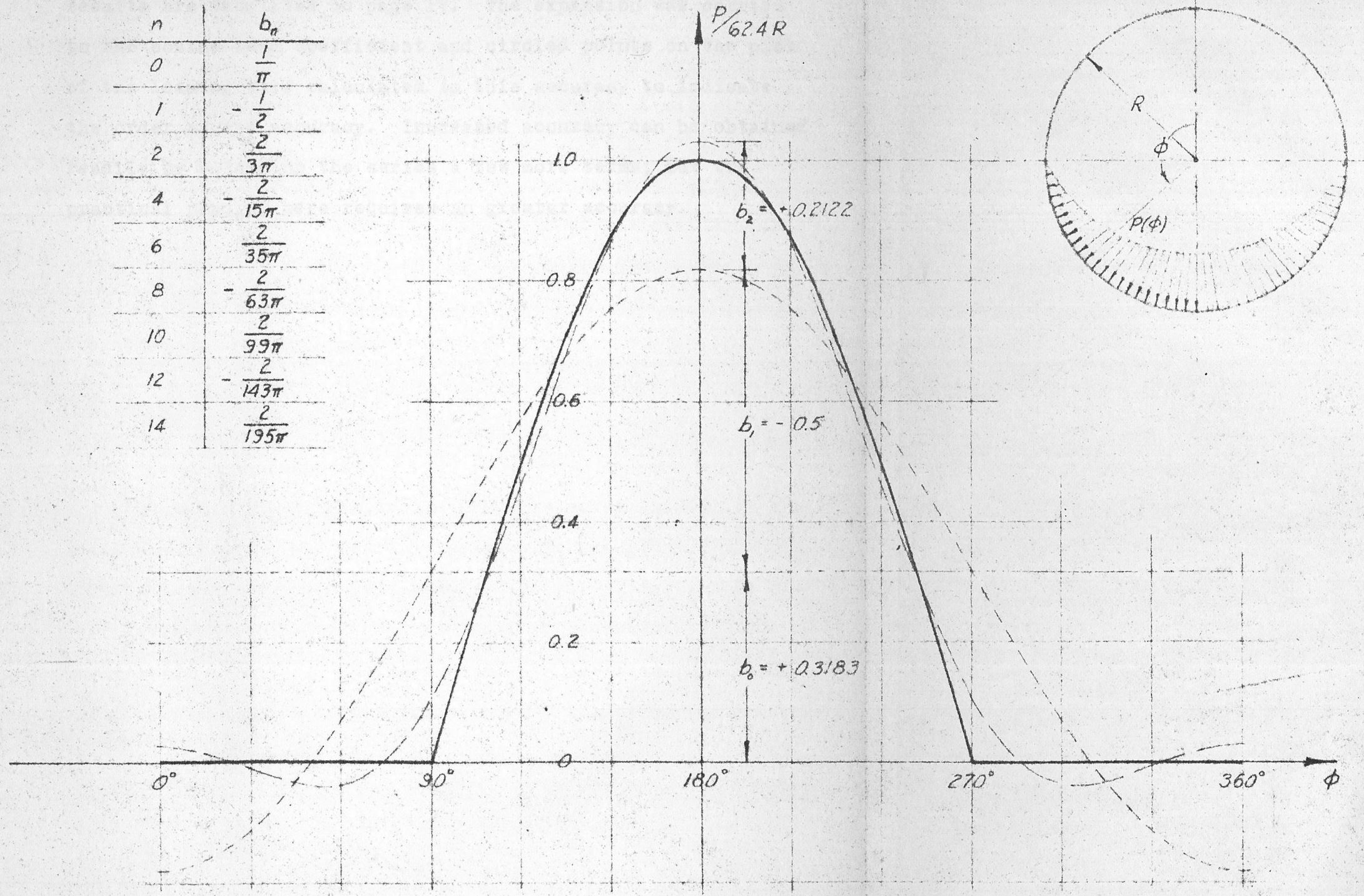

PRESSURE DISTRIBUTION

taken. The expansion has been solved in Appendix B and the results are tabulated on page 17. The expansion was carried to the cosine 14ϕ coefficient and circled points on the plot of the loading were calculated to this accuracy to indicate the order of the accuracy. Increased accuracy can be obtained readily by extending the series a few more terms; but the practical problem here requires no greater accuracy.

IV. CYLINDRICAL SECTION

When bolted into place, the eighteen-foot-long working section becomes a continuous beam, and it is best analyzed as having built-in ends. The actual mechanics of removing this section and of sealing it have been given considerable thought, but a discussion of possible procedures is out of place at this point. The actual analysis of the cylindrical section has been divided under the two design conditions into (1) a determination of member sizes and (2) a check of secondary stresses and stability.

Maximum-Head Condition:

Primary Shell Stresses:

The high static head design pressure makes the use of membrane theory quite satisfactory everywhere except near the supporting rings. The membrane theory for cylindrical shells has been developed without too much detail by Timoshenko[3]. The basic loads are all in the surface of the shell as indicated in the element under consideration in the following sketch:

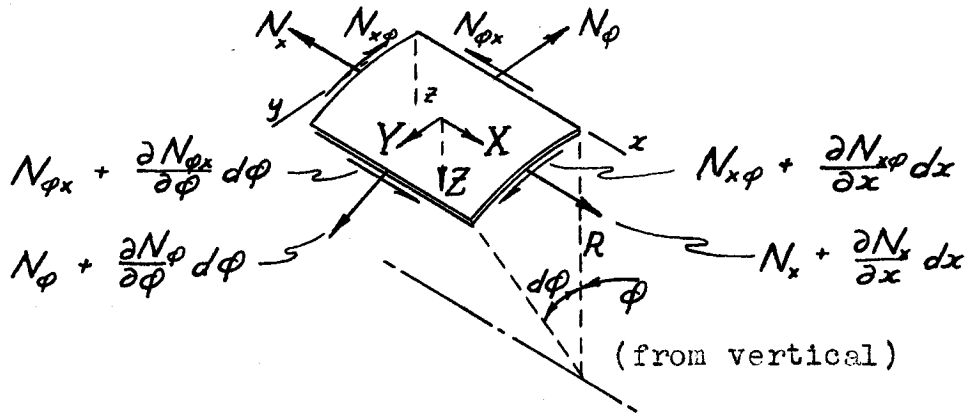

The basic equations of equilibrium are given as (224) on page 384 of the reference:

$$\frac{\partial N_x}{\partial x} + \frac{1}{R}\cdot\frac{\partial N_{x\varphi}}{\partial \varphi} = -X,$$

$$\frac{\partial N_{x\varphi}}{\partial x} + \frac{1}{R}\cdot\frac{\partial N_{\varphi}}{\partial \varphi} = -Y,$$

$$N_{\varphi} = -ZR.$$

Under fluid pressure, X = Y = 0 and the normal force,

$$Z = \gamma(-H_o + R\cos\varphi).$$

This gives the partial solution:

$$N_{\varphi} = \gamma R(H_o - R\cos\varphi),$$

$$N_{x\varphi} = -\gamma R x \sin\varphi + C_1(\varphi),$$

$$N_x = \frac{\gamma}{2}x^2\cos\varphi - \frac{x}{R}\cdot\frac{d}{d\varphi}C_1(\varphi) + C_2(\varphi).$$

Note that N_{φ} is neither a function of x nor everywhere equal to zero.

The fixed-end boundary condition requires that N_{φ} = 0 at both ends but the above solution does not yield this result. However, it is understood that the membrane theory will not hold near the supports and local secondary stresses have been considered in the next part of this sub-section (see p. 24). Since the flange is not infinitely rigid, there will be some circumferential stretching; and it turns out that the resulting N_{φ} value is more nearly correct than the zero value for this particular design. Further, the effect of these second-

ary stresses is shown to die out within less than two feet of the flange.

It remains to evaluate the two constants of integration from the boundary conditions. The condition that maximum shears be equal and opposite at the two ends of the tube gives:

$$C_1(\varphi) = \frac{\gamma}{2} R \ell \sin\varphi ;$$

and the fixed-end condition that the lengths of element lines remain constant yields:

$$\int_0^{\ell} (N_x - \nu N_\varphi)\, dx = 0 \quad \text{and}$$

$$C_2(\varphi) = \gamma\left[\nu R H_0 + \left(\frac{\ell^2}{12} - \nu R^2\right)\cos\varphi\right].$$

The final expressions for the running loads are:

$$\begin{cases} N_\varphi = \gamma R^2\left(\frac{H_0}{R} - \cos\varphi\right) & (1) \\ N_{x\varphi} = \frac{\gamma}{2} R\ell\left(1 - 2\frac{x}{\ell}\right)\sin\varphi & (2) \\ N_x = \frac{\gamma}{2}\ell^2\left(\frac{x^2}{\ell^2} - \frac{x}{\ell} + \frac{1}{6} - 2\nu\frac{R^2}{\ell^2}\right)\cos\varphi + \gamma\nu R H_0 & (3) \end{cases}$$

Turning to the particular section and fluid under consideration here, the following physical constants are applicable:

Density of water, $\gamma = 62.4\ ^{lb.}/_{ft.^3}$

$H_0 = 600$ ft. $\qquad R = 5$ ft.

$\nu = 0.3 \qquad \ell = 18$ ft.

Thus, the section to be considered looks like the following:

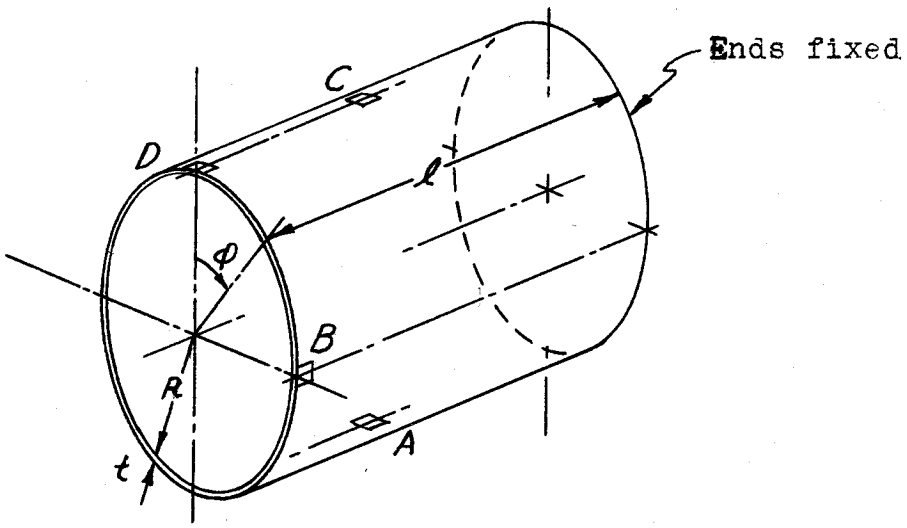

Note the directions of the x and ϕ coordinates.

Substituting the physical constants, the final stress state equations are:

$$\begin{cases} N_\phi = 130\ \frac{lb.}{in.}\,(120 - \cos\phi), \\ N_{x\phi} = 234\ \frac{lb.}{in.}\,(1 - \frac{x}{9ft.})\sin\phi, \\ N_x = 842.4\ \frac{lb.}{in.}\left(\frac{x^2}{324ft^2} - \frac{x}{18ft.} + .12037\right)\cos\phi + 4680\ \frac{lb.}{in.} \end{cases}$$

Investigating the critical locations, A, B, and C, indicated on the figure, the stress state at each point is found to be:

Location A --

$$N_\phi = 130\ \frac{lb.}{in.}\,(120 + 1) = 15.73\ \frac{kips}{in.},$$

$$N_{x\phi} = 0,$$

$$N_x = 842\ \frac{lb.}{in.}\left(\frac{1}{4} - \frac{1}{2} + .12\right)(-1) + 4680\ \frac{lb.}{in.} = 4.79\ \frac{kips}{in.}$$

$$\begin{cases} \text{Tension max.} = N_\phi = 15.73\ \frac{kips}{in.} \\ \text{Shear max.} = \frac{1}{2}(N_\phi - N_x) = 5.47\ \frac{kips}{in.} \end{cases}$$

Location B --

$$N_\varphi = 130\,\tfrac{lb.}{in.}(120+0) = 15.60\,\tfrac{kips}{in.}$$ - flange effect

$$N_{x\varphi} = 234\,\tfrac{lb.}{in.}(1-0) = 0.234\,\tfrac{kips}{in.}$$

$$N_x = 0 + 4680\,\tfrac{lb.}{in.} = 4.68\,\tfrac{kips}{in.}$$ ± secondary bending

$$\begin{cases} \text{Tension max.} = \dfrac{N_\varphi + N_x}{2} + \sqrt{\left(\dfrac{N_\varphi - N_x}{2}\right)^2 + N_{x\varphi}^2} = 15.61\,\tfrac{kips}{in.} - \\ \text{Shear max.} = \sqrt{\left(\dfrac{N_\varphi - N_x}{2}\right)^2 + N_{x\varphi}^2} = 5.47\,\tfrac{kips}{in.} - \end{cases}$$

Location C --

$$N_\varphi = 130\,\tfrac{lb.}{in.}(120-1) = 15.47\,\tfrac{kips}{in.}$$

$$N_{x\varphi} = 0$$

$$N_x = 842\,\tfrac{lb.}{in.}\left(\tfrac{1}{4} - \tfrac{1}{2} + .12\right)(+1) + 4680\,\tfrac{lb}{in.} = 4.57\,\tfrac{kips}{in.}$$

$$\begin{cases} \text{Tension max.} \approx N_\varphi = 15.47\,\tfrac{kips}{in.} \\ \text{Shear max.} \approx \tfrac{1}{2}(N_\varphi - N_x) = 5.45\,\tfrac{kips}{in.} \end{cases}$$

Thus it appears that the maximum running tension load of 15.73 kips per inch can be used to determine the required plate thickness.

The usual allowable tensile stress for structural grade steel is 18 k.s.i.; so applying this to the given running load, we get a plate thickness,

$$t = \frac{15.73\ k./in.}{18\ ksi} = 0.874\ in.\ (\text{say } \tfrac{7}{8}\ in).$$

To get an idea of the margin of safety this represents, the A.I.S.C.[4] gives the average ultimate tensile strength as

66 k.s.i. and shear ultimate as 3/4 of tensile; and the stress ratios are:

$$R_t = \frac{18\ ksi.}{66\ ksi.} = 0.273 \text{ for tension, and}$$

$$R_s = \frac{6.25\ ksi.}{49.5\ ksi.} = 0.126 \text{ for shear.}$$

The Army-Navy-Civil Committee on Aircraft Requirements[5] indicates that the margin of safety for such loadings can be expressed as:

$$M.S. = \frac{1}{R} - 1 = \begin{cases} 2.67 \text{ in tension,} \\ 6.92 \text{ in shear.} \end{cases}$$

This appears to be quite satisfactory -- particularly since the design load is the instantaneous peak of pressure under the impact of closing valves.

Secondary Stresses at Flanges:

Considering a flange of cross section A_f which exerts a load P per unit of circumference on the cylinder, the methods of section 82 of Plates and Shells[3] (p. 395 et seq.) are found to be applicable. Consider the pipe under pressure equivalent to the maximum average head, H_o, and use the notation indicated in the diagram:

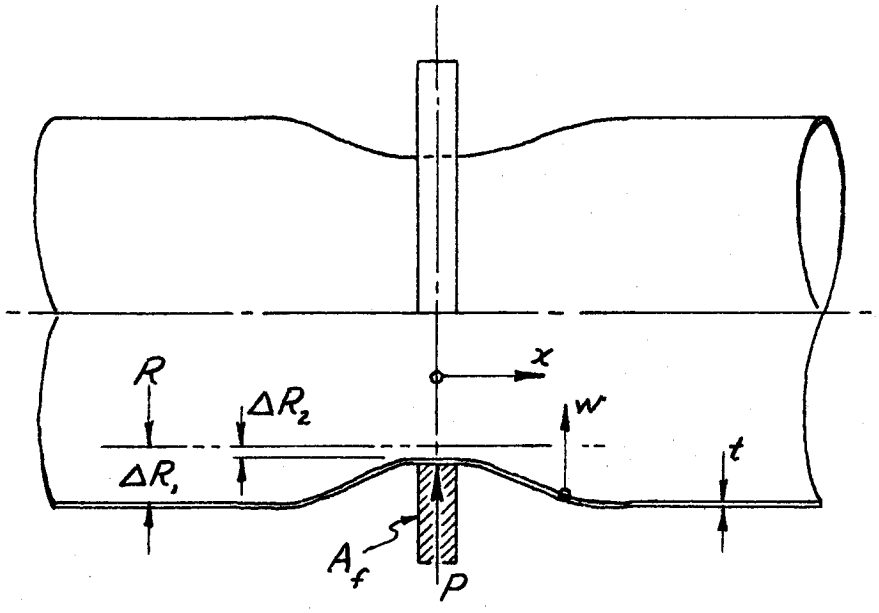

Based on circumferential stretching, the radial deflections are:

$$\Delta R_1 = \frac{\sigma}{E} R = \frac{18\,ksi.}{29000\,ksi.} \cdot 60\,in. = 0.0372\,in.$$

$$\Delta R_2 = \frac{\sigma_f}{E} R = \frac{PR^2}{EA_f} = 0.124 \cdot \frac{P}{A_f} \cdot \frac{in.^4}{kips}$$

Timoshenko uses the notation:

$$D = \frac{Et^3}{12(1-\nu^2)} = \frac{29000\,ksi\,(.875\,in.)^3}{12 \cdot 0.91} = 1779\,in.\,kips$$

$$\beta = \frac{Et}{4R^2D} = \frac{\sqrt[4]{3(1-\nu^2)}}{\sqrt{Rt}} = \frac{\sqrt[4]{3 \cdot 0.91}}{\sqrt{60in. \cdot .875in.}} = \frac{0.1774}{in.}$$

The β corresponds to the factor Z used by Schorer[6] in his paper on the "Design of Large Pipe Lines." The problem has been solved by Timoshenko with the following deflections under the ring lead point:

$$w_o = \frac{P}{8\beta^3 D} = \frac{P\,in./kip}{8(.1774)^3 1779} = \frac{P\,in.^2}{79.5\,kips}$$

Also, $w_o = \Delta R_1 - \Delta R_2 = 0.0372\,in - 0.124 \frac{P}{A_f} \cdot \frac{in.^4}{kips}$ from the elastic characteristics of the pipe and the flange. Therefore:

$$P = \frac{2.96 A_f}{9.86 in.^2 + A_f} \cdot \frac{kips}{in.}$$

and from Timoshenko's derivation:

$$M_o = \frac{P}{4\beta} = \frac{4.17 A_f}{9.86 in.^2 + A_f} \cdot \frac{in.-kips}{in.}$$

Furthermore, the effect of this flange dies out in a distance:

$$x = \frac{5\pi}{4\beta} = \frac{3.927 in.}{.1774} = 22 \text{ inches}$$

Now primary stresses at location D (see diagram on page 22) may be:

$$\sigma_x = \frac{N_x}{t} = \frac{842 lb.}{.875 in.^2} \cdot .12 + \frac{46801b.}{.875 in.^2} = 5.46 ksi$$

Considering 18 ksi to be the allowable total stress, this leaves 12.54 ksi for the allowable bending stress:

$$\sigma_{M_o} = M_o \frac{6}{t^2} = M_o \frac{7.837}{in.} = 12.54 ksi$$

Therefore, the largest allowable bending moment from this consideration can be equated to the M_o calculated as a function of the flange area; and the stiffest allowable flange can then be calculated thus:

$$M_o = \frac{12.54 in.-k.}{7.837 in.} = \frac{4.168 A_f}{9.86 in^2 + A_f} \cdot \frac{in.-k.}{in.}$$

$$A_f = \frac{1.6 \cdot 9.86 in.^2}{2.568} = 6.14 in.^2$$

Hoop stresses in the flange will be given by:

$$\sigma_f = \frac{0.12 in.^4}{kips} \cdot \frac{EP}{RA_f} = 11.09 ksi$$

The problem of bending stresses in the flange will be con-

sidered under the following loads:

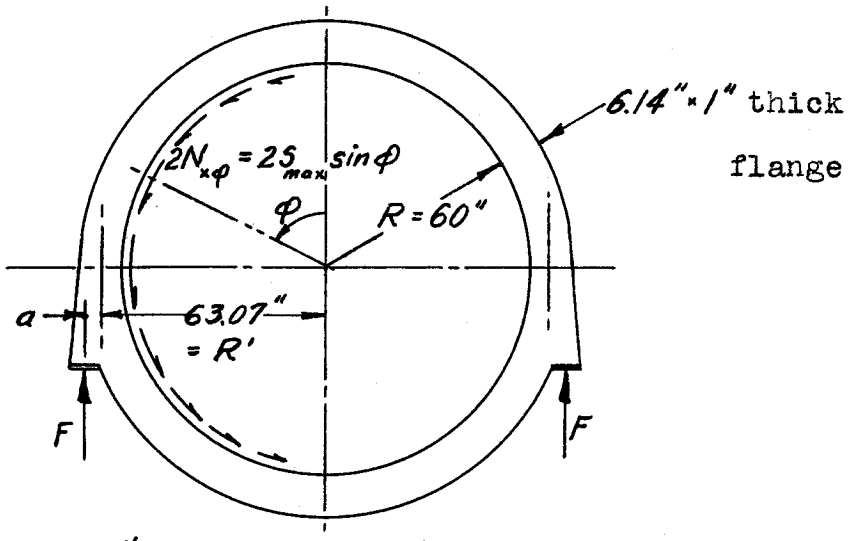

$$F = \tfrac{1}{2} \cdot 62.4 \tfrac{lb.}{ft.^3} \cdot 78.5\ ft^2 \cdot 18\ ft. = 44.11\ kips$$

$$= 2RS_{max.} \int_0^{\pi} \sin^2\varphi\, d\varphi = 60in.\ \pi\ S_{max.}$$

$S_{max.} = 0.234 \tfrac{kips}{in.}$ -- which checks.

Schorer[6] has solved the bending moment problem for most efficient placing of the supporting reactions; and his solution yields:

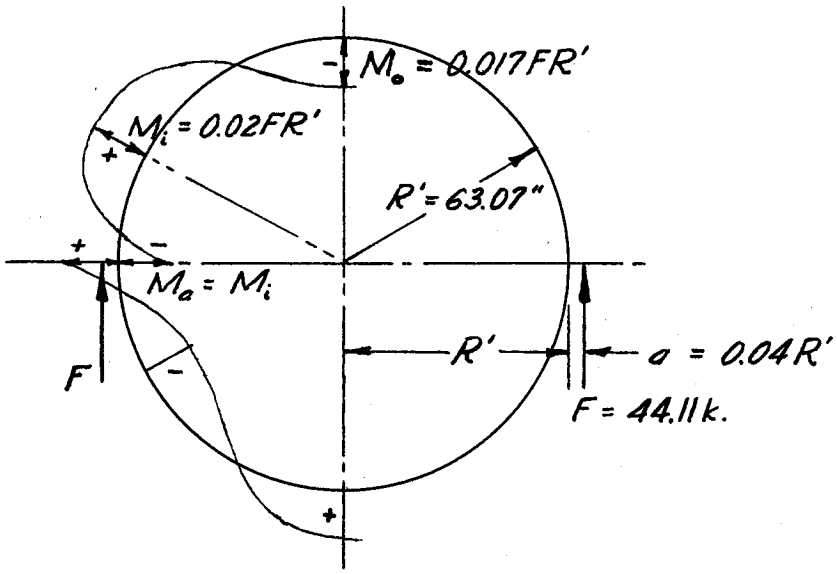

$a = 0.04R' = 2.52\ in.$

$M_{max.} = 0.02FR' = 1.26in. \times 44.11k. = 55.58\ in.\text{-}kips.$

Checking the stresses in a 6.14 in. x 1 in. flange, the section modulus,

$$Z = \frac{1\,in.(6.14\,in.)^2}{6} = 6.3\,in.^3$$

$$\sigma_b = \frac{M}{Z} = \frac{55.6\,in.-k.}{6.3\,in.^3} = 8.82\,ksi.$$

Combined stresses in the flange give:

$$\sigma_{max.} = \sigma_f + \sigma_b = 11.09\,ksi. + 8.82\,ksi. = 19.9\,ksi.$$

This is not too high since the pipe itself restrains this bending to a certain extent.

Part-Full Condition:

Primary Shell Stresses:

The part-full condition gives little support to the shell; so shears and bending moments across the sheet become important. Actually, circumferential shears and moments are of more consequence than longitudinal or torsional moments; but all of these effects have been included. The problem of whether the secondary effects of local deformation are negligible or not is to be established; and Timoshenko[3] (p. 439) states that they are negligible if N_x, N_φ, and $N_{x\varphi}$ are small in comparison with their critical buckling values for the shell.

To establish the negligibility of local deformations, consider the following over-simplified analysis:

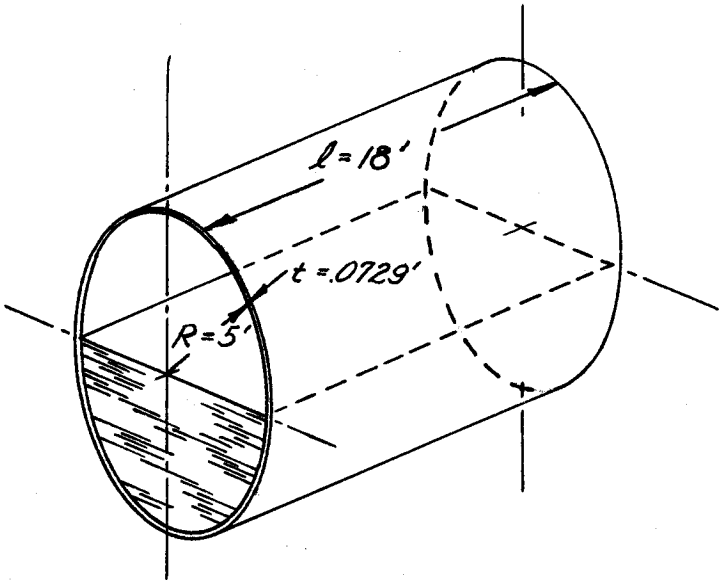

Weight / ft. = $62.4 \frac{lb.}{ft.^3} \cdot 39.27 ft.^2 + 35.7 \frac{lb.}{ft.^2} \cdot 31.42 ft. = 3.572 \frac{kips}{ft.}$

Max. moment = $\frac{wl^2}{12} = \frac{3.572 \frac{kips}{ft.}}{12} (18ft.)^2 = 96.45$ ft.-kips

Max. shear = $\frac{wl}{2} = \frac{3.572 \frac{kips}{ft.}}{2} \cdot 18 ft. = 32.15$ kips

Approximate maximum stresses over supports:

Compression = $\frac{M}{\pi R^2 t} = \frac{96.45 ft.-kips}{\pi 25 ft^2 .0729 ft.} = 117$ psi.

Shear = $\frac{0.3535 V}{Rt} = \frac{.3535 \cdot 32.15 kips}{5 ft. \cdot .0729 ft.} = 216$ psi.

Approximate buckling stresses:

(7) $\sigma_{cr} = E\left[9\left(\frac{t}{R}\right)^{1.6} + 0.16\left(\frac{t}{l}\right)^{1.3}\right] = 29 \times 10^6 psi. \cdot .0105 = 304\,000$ psi.

(8) $\tau_{cr} = \frac{0.2357 E}{(1-\nu^2)^{3/4}} \left(\frac{t}{R}\right)^{\frac{3}{2}} = 7336 ksi (.0146)^{\frac{3}{2}} = 12\,934$ psi.

Obviously the approximate stresses are very much lower than the probable minimum buckling stresses, particularly since the max-

imum shear indicated is at the ring supports where buckling is not a problem.

The shears and moments to be considered in addition to those in the surface of the shell (see figure on p. 19) are indicated in the following illustration:

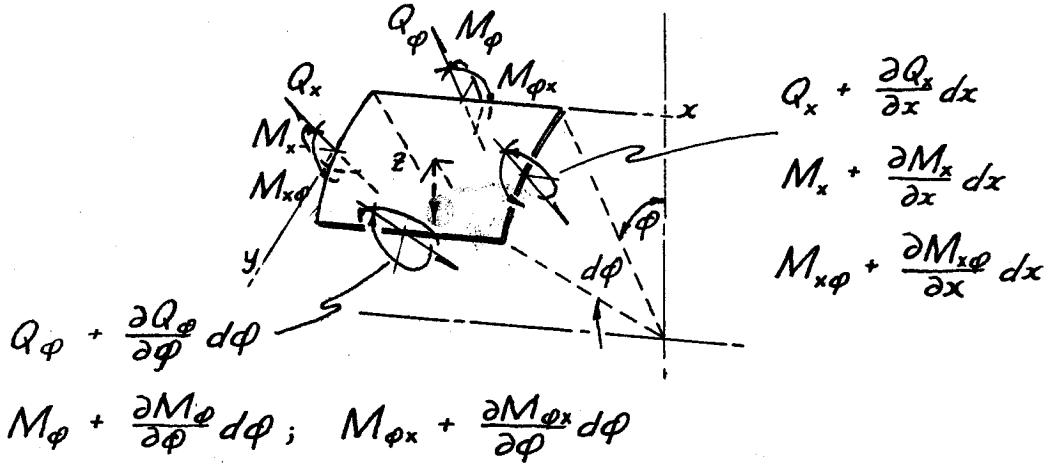

Section 88 of Theory of Plates and Shells (p. 433 et seq.) derives the general equilibrium equations for this element; and equations (255), page 440, are the form they take with the simplification of small deflections:

$$\begin{cases} R \cdot \frac{\partial N_x}{\partial x} + \frac{\partial N_{\varphi x}}{\partial \varphi} = -XR = 0 \\ \frac{\partial N_\varphi}{\partial \varphi} + R \cdot \frac{\partial N_{x\varphi}}{\partial x} - Q_\varphi = -YR = -178.5 \frac{lb.}{ft.} \sin\varphi \\ R \cdot \frac{\partial Q_x}{\partial x} + \frac{\partial Q_\varphi}{\partial \varphi} + N_\varphi = -ZR = -178.5 \frac{lb.}{ft.} \cos\varphi + \\ \qquad + 1560 \frac{lb.}{ft.} \sum_{n=0}^{\infty} b_n^* \cos n\varphi . \\ R \cdot \frac{\partial M_{x\varphi}}{\partial x} - \frac{\partial M_\varphi}{\partial \varphi} + RQ_\varphi = MR = 0 \\ \frac{\partial M_{\varphi x}}{\partial \varphi} + R \cdot \frac{\partial M_x}{\partial x} - RQ_x = M'R = 0 \end{cases}$$

*See page 17 and Appendix B for values of b_n to be used.

Q_x and Q_φ can be eliminated from the above equations; and the remaining forces and moments can be expressed in terms of the displacements u, v and w. That is, elastic considerations given in Plates and Shells, pages 354 and 439, equations (207), (208) and (254), yield:

$$N_x = \frac{12D}{t^2}\left(\frac{\partial u}{\partial x} + \frac{\nu}{R}\cdot\frac{\partial v}{\partial \varphi} - \frac{\nu}{R}\cdot w\right)$$

$$N_\varphi = \frac{12D}{t^2}\left(\nu\cdot\frac{\partial u}{\partial x} + \frac{1}{R}\cdot\frac{\partial v}{\partial \varphi} - \frac{w}{R}\right)$$

$$N_{x\varphi} = N_{\varphi x} = \frac{12D}{t^2}\left(\frac{1-\nu}{2}\right)\left(\frac{1}{R}\cdot\frac{\partial u}{\partial \varphi} + \frac{\partial v}{\partial x}\right)$$

$$M_x = \frac{12D}{t^2}\left(-\frac{t^2}{12}\right)\left(\frac{\nu}{R^2}\cdot\frac{\partial v}{\partial \varphi} + \frac{\partial^2 w}{\partial x^2} + \frac{\nu}{R^2}\cdot\frac{\partial^2 w}{\partial \varphi^2}\right)$$

$$M_\varphi = \frac{12D}{t^2}\left(-\frac{t^2}{12}\right)\left(\frac{1}{R^2}\cdot\frac{\partial v}{\partial \varphi} + \nu\frac{\partial^2 w}{\partial x^2} + \frac{1}{R^2}\cdot\frac{\partial^2 w}{\partial \varphi^2}\right)$$

$$M_{x\varphi} = -M_{\varphi x} = \frac{12D}{t^2}\left[\frac{t^2(1-\nu)}{12R}\right]\left(\frac{\partial v}{\partial x} + \frac{\partial^2 w}{\partial x\,\partial \varphi}\right)$$

The given equations are combined on page 440 to three equations (257) in three unknown displacements:

$$\begin{cases} R\cdot\dfrac{\partial^2 u}{\partial x^2} + \dfrac{1-\nu}{2R}\cdot\dfrac{\partial^2 u}{\partial \varphi^2} + \dfrac{1+\nu}{2}\cdot\dfrac{\partial^2 v}{\partial x\,\partial \varphi} - \nu\cdot\dfrac{\partial w}{\partial x} = 0 \\ \dfrac{1+\nu}{2}\cdot\dfrac{\partial^2 u}{\partial x\,\partial \varphi} + R\cdot\dfrac{1-\nu}{2}\cdot\dfrac{\partial^2 v}{\partial x^2} + \dfrac{1}{R}\cdot\dfrac{\partial^2 v}{\partial \varphi^2} - \dfrac{1}{R}\cdot\dfrac{\partial w}{\partial \varphi} + \dfrac{t^2}{12R}\left[(1-\nu)\dfrac{\partial^2 v}{\partial x^2}\right. \\ \qquad \left. + \dfrac{1}{R^2}\cdot\dfrac{\partial^2 v}{\partial \varphi^2} - \dfrac{\partial^3 w}{\partial x^2\,\partial \varphi} + \dfrac{1}{R^2}\cdot\dfrac{\partial^3 w}{\partial \varphi^3}\right] = -14.9\,\dfrac{lb.}{ft.}\,\dfrac{t^2}{D}\sin\varphi \\ \nu\cdot\dfrac{\partial u}{\partial x} + \dfrac{1}{R}\cdot\dfrac{\partial v}{\partial \varphi} - \dfrac{w}{R} - \dfrac{t^2}{12R}\left[(2-\nu)\dfrac{\partial^3 v}{\partial x^2\,\partial \varphi} + \dfrac{1}{R^2}\cdot\dfrac{\partial^3 v}{\partial \varphi^3} + R^2\dfrac{\partial^4 w}{\partial x^4} + \right. \end{cases}$$

$$\left[+2\frac{\partial^4 w}{\partial x^2 \partial \phi^2} + \frac{1}{R^2}\cdot\frac{\partial^4 w}{\partial \phi^4} \right] = -14.9\ \frac{lb.}{ft.}\ \frac{t^2}{D}\cos\phi + 130\ \frac{lb.}{ft.}\cdot\frac{t^2}{D}\sum_{n=0}^{\infty} b_n \cos n\phi.$$

Fixed ends and symmetry about the vertical center line give the displacements the following forms; which are now assumed as solutions with the coefficients to be evaluated:

$$u = \sum\sum A_{mn} \cos n\phi \sin\frac{2m\pi x}{l}$$

$$v = \sum\sum B_{mn} \sin n\phi \sin\frac{m\pi x}{l}$$

$$w = \sum\sum C_{mn} \cos n\phi \sin\frac{m\pi x}{l}$$

Also, the physical constants which appear in the various equations must be introduced to reduce the problem to a numerical one; and these constants are:

$$\nu = 0.3,\quad t = 0.0729\ ft.,\quad R = 5\ ft.,\quad l = 18\ ft.$$

$$\frac{t^2}{D} = \frac{12(1-\nu)}{tE} = \frac{8}{29}\times 10^{-7}\ \frac{ft.}{lb.}$$

$$\frac{t^2}{12R} = \frac{49\ ft.}{552{,}960} = 0.886\times 10^{-4}\ ft.$$

The relations of the preceding paragraph substitute into the three displacement equations to give for solution:

$$\sum\sum 11.634(m^2 + .1149n^2) A_{mn} \cos n\phi \sin\frac{2mx}{5.73\ ft.} + \sum\sum m(C_{mn} - 2.1667n B_{mn}) \cos n\phi \cos\frac{mx}{5.73\ ft.} = 0 \qquad (1)$$

$$\sum\sum 8403\, mn\, A_{mn} \sin n\phi \cos \frac{2mx}{5.73 ft.} + \sum\sum [19744(m^2 + 3.751n^2) B_{mn} - n(m^2 + 74074 + 32.815n^2) C_{mn}] \sin n\phi \sin \frac{mx}{5.73 ft.} =$$

$$= 0.15200 ft. \sin \phi \qquad (2)$$

$$\sum\sum 50934\, m A_{mn} \cos n\phi \cos \frac{2mx}{5.73 ft.} + \sum\sum [2.2315n(m^2 + 43592 + 0.7725n^2) B_{mn} - (m^4 + 2.6255m^2n^2 + 1.7237n^4 + 97278) C_{mn}] \cdot \cos n\phi \sin \frac{mx}{5.73 ft.} = ft.(0.5552 - 1.0717 \cos \phi + 0.37015 \cos 2\phi - 0.07403 \cos 4\phi + 0.03172 \cos 6\phi - 0.01763 \cos 8\phi + 0.01122 \cos 10\phi - 0.00776 \cos 12\phi + 0.00574 \cos 14\phi - \cdots) \qquad (3)$$

These equations have been solved in Appendix C and the values of the coefficients are tabulated on the next sheet. The values in the table are in billionths of a foot; and in order to get an idea of the cumulative effect, the transverse deflections of the shell were calculated at the four points indicated in the figure below:

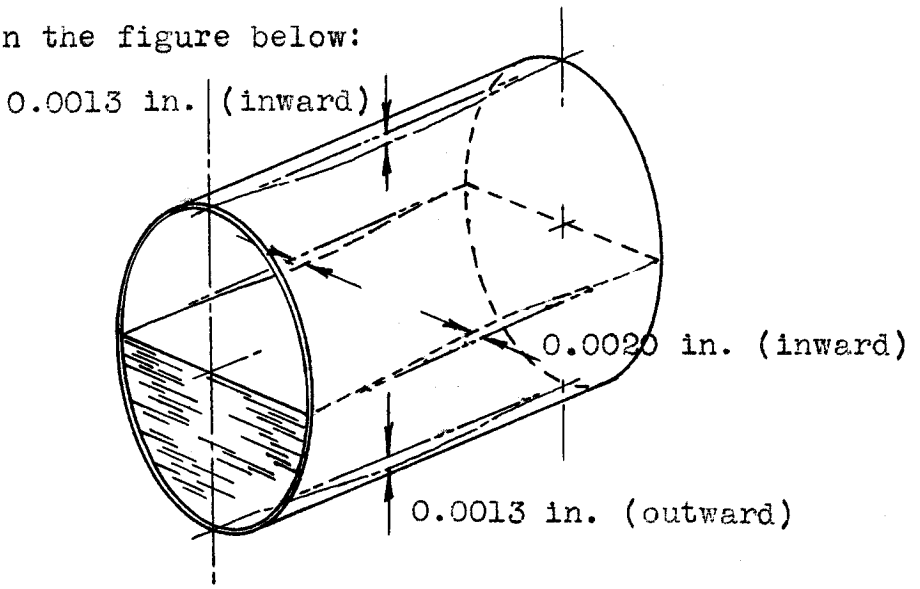

Values of $C_{mn} \cdot 10^9$ in feet:

m	n = 0	1	2	4	6	8	10	12	14
1	- 7 260	76 570	- 79 491	69 715	- 28 428	4 721	- 1 077	331	- 125
3	- 2 420	6 979	- 4 300	2 432	- 1 752	798	- 271	96	
5	- 1 444	3 279	- 1 530	625	- 426	296	- 109	45	
7	- 1 013	2 127	- 871	280	- 171	101	- 52		
9	- 764	1 533	- 585	159	- 87	50			
11	- 527	1 141	- 418	101	- 50				
13	- 432	849	- 303	67					
15	- 319	621	- 218	46					
17	- 230	442	- 155						
19	- 163	314	- 109						
21	- 115	222	- 77						
23	- 82	157	- 54						
25	- 58	112							
27		80							
29		58							

Values of $B_{mn} \cdot 10^9$ in feet:

m	n = 1	2	4	6	8	10	12
1	62 546	- 37 336	17 268	- 4 779	605	- 112	12
3	2 311	- 1 347	533	- 278	99	- 28	
5	496	- 288	111	- 61	34		
7	178	- 101	39	- 21			
9	81	- 46	17				
11	42	- 23					
13	23						

The necessity for zero u-displacement at the ends (fixity) and in the middle (anti-symmetry) results in zero throughout the length under the trigonometric expansions of the loading as sines of odd multiples; that is, all A coefficients are zero. Thus it can be stated that transverse plane sections remain plane and vertical That sections remain plane is a basic assumption of simple beam theory; but to keep those planes vertical requires restraints which nullify the axial bending stresses without necessarily disturbing the shear distribution. Therefore, the axial bending stresses calculated from simple theory must be added to the following results for N_x; and Poisson effect of these stresses must be combined with the N_φ results. The $N_{x\varphi}$ results should check reasonably well with simple theory and their accuracy should be indicative of accuracy of the solution generally.

Since all of the A coefficients are zero and the x-displacements are restrained to $u(x,\varphi) = 0$, the expressions for the stress (actually running-load) state throughout the shell can be simplified to the following form:

$$N_x = \frac{12\nu D}{Rt^2}\left(\frac{\partial v}{\partial \varphi} - w\right),$$

$$N_\varphi = \frac{12D}{Rt^2}\left(\frac{\partial v}{\partial \varphi} - w\right),$$

$$N_{x\varphi} = N_{\varphi x} = \frac{6D}{t^2}(1-\nu)\frac{\partial v}{\partial x},$$

$$M_x = -\frac{\nu D}{R^2}\left(\frac{\partial v}{\partial \varphi} + \frac{R^2}{\nu}\cdot\frac{\partial^2 w}{\partial x^2} + \frac{\partial^2 w}{\partial \varphi^2}\right),$$

$$M_\varphi = -\frac{D}{R^2}\left(\frac{\partial v}{\partial \varphi} + \nu R^2 \frac{\partial^2 w}{\partial x^2} + \frac{\partial^2 w}{\partial \varphi^2}\right),$$

$$M_{x\varphi} = -M_{\varphi x} = \frac{D}{R}(1-\nu)\left(\frac{\partial v}{\partial x} - \frac{\partial^2 w}{\partial x\,\partial \varphi}\right).$$

From the previous discussion, it can be seen that the chief contribution of these determinations in comparison with simple beam theory will be the hoop tensions and the transverse bending moments. Since no exact theory of buckling exists for these loadings, only the order of magnitudes are necessary to verify their insignificance.

Substituting the final solutions for v and w into the above equations, the expressions for running load become:

$$N_x = 2175 \frac{kips}{in.} \sum_{m=1}^{\infty}\sum_{n=0}^{\infty} (nB_{mn} - C_{mn}) \cos n\varphi \sin \frac{m\pi x}{\ell},$$

$$N_\varphi = 7250 \frac{kips}{in.} \sum_{m=1}^{\infty}\sum_{n=0}^{\infty} (nB_{mn} - C_{mn}) \cos n\varphi \sin \frac{m\pi x}{\ell},$$

$$N_{x\varphi} = 2214 \frac{kips}{in.} \sum_{m=1}^{\infty}\sum_{n=1}^{\infty} mB_{mn} \sin n\varphi \cos \frac{m\pi x}{\ell},$$

$$M_x = 1.779 \frac{in.-k.}{in.} \sum_{m=1}^{\infty}\sum_{n=0}^{\infty} \left[-nB_{mn} + (2.538m^2 + n^2)C_{mn}\right] \cdot \cos n\varphi \sin \frac{m\pi x}{\ell},$$

$$M_\varphi = 5.930 \frac{in.-k.}{in.} \sum_{m=1}^{\infty}\sum_{n=0}^{\infty} \left[-nB_{mn} + (0.2284m^2 + n^2)C_{mn}\right] \cdot \cos n\varphi \sin \frac{m\pi x}{\ell},$$

$$M_{x\phi} = 3.622 \frac{\text{in.-k.}}{\text{in.}} \sum_{m=1}^{\infty}\sum_{n=0}^{\infty} m(B_{mn} - nC_{mn}) \sin n\phi \cos \frac{m\pi x}{\ell}.$$

Maximum stresses at the previously investigated locations (i.e., at points investigated under the high-head condition) are as follows:

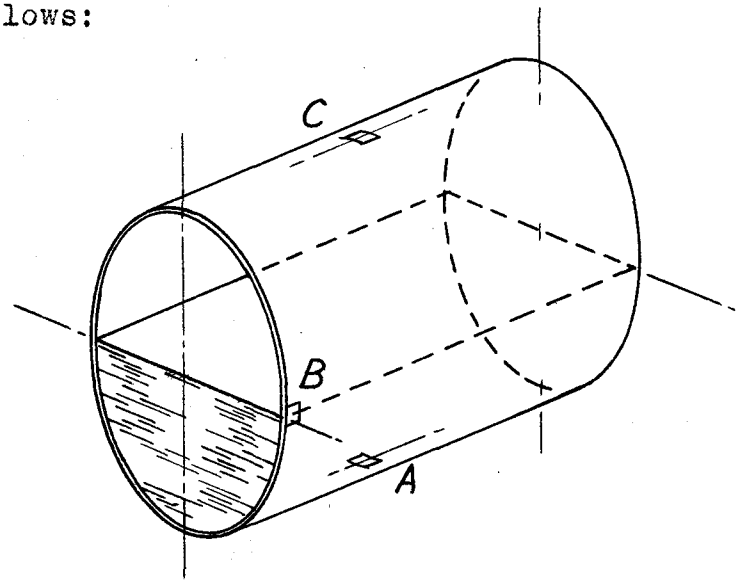

Location A--

$$N_x = 2175 \frac{\text{kips}}{\text{in.}} \sum_{m=1}^{\infty} \left[-C_{mo} - B_{m1} + C_{m1} + \sum_{n=2}^{\infty}(nB_{mn} - C_{mn})\right] \sin \frac{m\pi}{2}$$

$$= 43.6 \frac{\text{lb.}}{\text{in.}}; \text{ or } \sigma_x = \frac{N_x}{t} = 50 \text{ psi. } (+59 \text{ psi. from simple bending});$$

$$N_\phi = 7250 \frac{\text{kips}}{\text{in.}} \sum_{m=1}^{\infty} \left[-C_{mo} - B_{m1} + C_{m1} + \sum_{n=2}^{\infty}(nB_{mn} - C_{mn})\right] \sin \frac{m\pi}{2}$$

$$= 145.4 \frac{\text{lb.}}{\text{in.}}; \text{ or } \sigma_\phi = \frac{N_\phi}{t} = 166 \text{ psi. } (-18 \text{ psi. from simple bending});$$

$$N_{x\varphi} = M_{x\varphi} = 0;$$

$$M_x = 1.779\,\text{kips} \sum_{m=1}^{\infty} \Big\{ 2.538m^2 C_{mo} + B_{m1} - (2.538m^2+1)C_{m1} + \sum_{n=2}^{\infty} \big[(2.538m^2+n^2)C_{mn} - nB_{mn} \big] \Big\} \sin\frac{m\pi}{2} = -0.194 \frac{\text{in.-lb.}}{\text{in.}},$$

$$\text{or} \quad \sigma_{b\text{-}x} = \frac{6M_x}{t^2} = \pm 1.52\ \text{psi.};$$

$$M_\varphi = 5.930\,\text{kips} \sum_{m=1}^{\infty} \Big\{ 0.2284m^2 C_{mo} + B_{m1} - (0.2284m^2+1)C_{m1} + \sum_{n=2}^{\infty} \big[(0.2284m^2+n^2)C_{mn} - nB_{mn} \big] \Big\} \sin\frac{m\pi}{2} = 0.065 \frac{\text{in.-lb.}}{\text{in.}},$$

$$\text{or} \quad \sigma_{b\text{-}\varphi} = \frac{6M_\varphi}{t^2} = \pm 0.51\ \text{psi.}$$

Location B--

$$N_x = N_\varphi = 0;$$

$$N_{x\varphi} = 2214 \frac{\text{kips}}{\text{in.}} \sum_{m=1}^{\infty} mB_{m1} = 165 \frac{\text{lb.}}{\text{in.}}, \quad \text{or}$$

$$\tau_{x\varphi} = \frac{N_{x\varphi}}{t} = 189\ \text{psi.};$$

$$M_x = M_\varphi = 0;$$

$$M_{x\varphi} = -M_{\varphi x} = 3622\,\text{kips} \sum_{m=1}^{\infty} m(B_{m1} - C_{m1}) =$$

$$= 743 \frac{\text{in.-lb.}}{\text{in.}}, \quad \text{or} \quad \tau'_{x\varphi} = M_{x\varphi} \frac{3+0.9t}{8t^2}$$

$$= 459\ \text{psi.}$$

Location C--

$$N_x = 2175 \frac{kips}{in.} \sum_{m=1}^{\infty}\sum_{n=0}^{\infty}(nB_{mn} - C_{mn}) \sin\frac{m\pi}{2} = -4.4 \frac{lb.}{in.}, \text{ or}$$

$$\sigma_x = \frac{N_x}{t} = -5 psi. (-59 psi. \text{ from simple bending});$$

$$N_\varphi = 7250 \frac{kips}{in.} \sum_{m=1}^{\infty}\sum_{n=0}^{\infty}(nB_{mn} - C_{mn}) \sin\frac{m\pi}{2} = -14.5 \frac{lb.}{in.}, \text{ or}$$

$$\sigma_\varphi = \frac{N_\varphi}{t} = -17 psi. (+18 psi. \text{ from simple bending});$$

$$N_{x\varphi} = M_{x\varphi} = 0;$$

$$M_x = 1.779 kips \sum_{m=1}^{\infty}\sum_{n=0}^{\infty}[-nB_{mn} + (2.538m^2 + n^2)C_{mn}] \sin\frac{m\pi}{2} =$$

$$= 0.116 \frac{in.-lb.}{in.}, \quad \text{or} \quad \sigma_{b-x} = \frac{6M_x}{t^2} = 0.91 psi.;$$

$$M_\varphi = 5.930 kips \sum_{m=1}^{\infty}\sum_{n=0}^{\infty}[-nB_{mn} + (2.538m^2 + n^2)C_{mn}] \sin\frac{m\pi}{2} =$$

$$= 0.279 \frac{in.-lb.}{in.}, \quad \text{or} \quad \sigma_{b-\varphi} = \frac{6M_\varphi}{t^2} = 2.18 psi.$$

All of these stresses are seen to be extremely low and of little concern from a practical standpoint; but some comments are in order.

The maximum shear stress of 189 psi is off from the more accurate (for this shear determination) result from simple beam theory of 216 psi by only twelve per cent and this is a fair measure of the overall accuracy of the series solution

given here. Greater accuracy could be obtained by extending the series solutions further but no practical advantage would obtain. The calculations of transverse bending moments are somewhat less accurate because of the slow rates of convergence of their series. However, these moments are so small that there is no doubt about the needlessness of extending their series. The cylindrical section as proposed is definitely stable even under the part-full condition.

V. CONICAL SECTION

The conical diffuser section (B on page 6) is an eighteen-foot frustrum; and the end-conditions are such that they are properly considered fixed. The elements of the cone are inclined at only five degrees to the axis; so one would hope to apply the techniques used for the cylindrical section without too much difficulty. Actually, membrane theory has been applied for the high-head design condition without any additional simplifying assumptions.

Maximum-Head Condition:

Primary Shell Stresses:

The high design pressure for this condition again makes the use of membrane theory quite satisfactory everywhere except near the supporting rings. The only conical cases developed by Timoshenko[3] in his Plates and Shells (pp. 362-364) are not applicable to this particular problem. However, the basic equations can be set up by considering the following element of the surface with the notation as indicated:

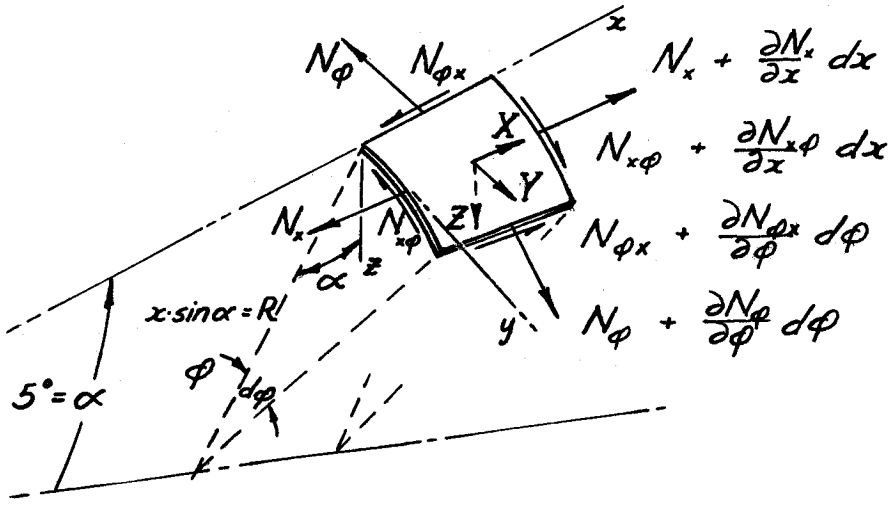

Equilibrium of the element in the x, y and z directions respectively gives the three equations which follow:

$$\frac{\partial N_x}{\partial x} dx(R\,d\phi) + N_x dx\left(\frac{R}{x} d\phi\right) + \frac{\partial N_{x\phi}}{\partial \phi} d\phi\, dx - N_\phi dx\left(\frac{R}{x} d\phi\right) =$$

$$= -X \cdot R\, d\phi\, dx = 0;$$

$$\frac{\partial N_{x\phi}}{\partial x} dx(R\,d\phi) + N_{x\phi} dx\left(\frac{R}{x} d\phi\right) + \frac{\partial N_\phi}{\partial \phi} d\phi\, dx = -Y \cdot R\, d\phi\, dx = 0;$$

$$\cos\alpha \cdot N_\phi\, dx\, d\phi = -Z \cdot R\, d\phi\, dx = \gamma R\, d\phi\, dx (H_o - R\cos\phi).$$

These simplify to the following expressions if R is replaced by $x \cdot \sin\alpha$:

$$\begin{cases} x \cdot \dfrac{\partial N_x}{\partial x} + N_x + \dfrac{1}{\sin\alpha} \cdot \dfrac{\partial N_{x\phi}}{\partial \phi} - N_\phi = 0, & (1) \\ x \cdot \dfrac{\partial N_{x\phi}}{\partial x} + N_{x\phi} + \dfrac{1}{\sin\alpha} \cdot \dfrac{\partial N_\phi}{\partial \phi} = 0, & (2) \\ N_\phi = \left(\dfrac{\gamma \sin^2\alpha}{\cos\alpha}\right) x \left(\dfrac{H_o}{\sin\alpha} - x \cdot \cos\phi\right). & (3) \end{cases}$$

Substituting equation (3) into (2) gives a partial differential equation which is "exact"; so the integration is performed quite readily, to give:

$$N_{x\phi} = -\frac{\gamma}{3} \tan\alpha \cdot x^2 \cdot \sin\phi + \frac{1}{x} \cdot C_1(\phi).$$

The boundary condition which evaluates the constant of integration here is that the total shear deflection from one end of an element to the other shall be zero. This is equivalent to saying in terms of the loading:

$$\int_{x_1}^{x_2} N_{x\phi}\, dx = 0, \qquad \text{which yields:}$$

$$C_1(\varphi) = \frac{\gamma}{3} \tan\alpha \frac{(x_2^3 - x_1^3)}{3 \ln \frac{x_2}{x_1}} \sin\varphi.$$

Therefore, the final expression for the shear state is:

$$N_{x\varphi} = -\left(\frac{\gamma}{3}\tan\alpha\right)\left[x^2 - \frac{(x_2^3 - x_1^3)}{x\, 3 \ln \frac{x_2}{x_1}}\right] \sin\varphi. \qquad (4)$$

Substituting equations (3) and (4) into equation (1) gives another "exact" differential equation of somewhat greater complexity. The solution is straightforward, however; and the result is:

$$N_x = \left(\frac{\gamma}{9\cos\alpha}\right)\left[x^2(1-3\sin^2\alpha) - \frac{\ln x}{x} \cdot \frac{(x_2^3 - x_1^3)}{\ln \frac{x_2}{x_1}}\right]\cos\varphi +$$
$$+ \left(\frac{\gamma H_0}{2}\tan\alpha\right)x + \frac{1}{x} C_2(\varphi).$$

The boundary condition here is that the elements shall have no net elongation over their length. This is expressed in terms of running loads as:

$$\int_{x_1}^{x_2} (N_x - \nu N_\varphi)\, dx = 0, \qquad \text{which yields:}$$

$$-C_2(\varphi) = \left(\frac{\gamma}{9\cos\alpha}\right)\left(\frac{x_2^3 - x_1^3}{\ln \frac{x_2}{x_1}}\right)\left[\frac{1}{3} - \sin^2\alpha(1-3\nu) - \left(\frac{\ln^2 x_2 - \ln x_1^2}{2 \ln \frac{x_2}{x_1}}\right)\right] \cdot$$
$$\cos\varphi + \left(\frac{\gamma H_0}{2}\tan\alpha\right)\left(\frac{x_2^2 - x_1^2}{\ln \frac{x_2}{x_1}}\right)\left(\frac{1}{2} - \nu\right).$$

Therefore, the final expression for longitudinal running load turns out to be:

$$N_x = \left(\frac{\gamma}{9\cos\alpha}\right)\left\{x^2(1-3\sin^2\alpha) - \frac{1}{x}\left(\frac{x_2^3 - x_1^3}{\ln \frac{x_2}{x_1}}\right)\left[\ln x + \frac{1}{3} - \right.\right.$$
$$\left.\left. - (1-3\nu)\sin^2\alpha - \left(\frac{\ln^2 x_2 - \ln^2 x_1}{2 \ln \frac{x_2}{x_1}}\right)\right]\right\}\cos\varphi + \left(\frac{\gamma H_0}{2}\tan\alpha\right) \cdot$$
$$\cdot \left[x - \left(\frac{\frac{1}{2} - \nu}{x}\right)\left(\frac{x_2^2 - x_1^2}{\ln \frac{x_2}{x_1}}\right)\right]. \qquad (5)$$

It is to be remembered here that although the distance between end rings has been maintained constant, no provision has been made in the equations for taking out the axial thrust resultant. Therefore, this might be considered as being similar to the conical end of a boiler where the tension increases as one moves away from the apex.

The correction for boiler effect can be taken directly from Timoshenko[3], Plates and Shells (p. 363, fig. 142a & b). As indicated there, the cases to be superimposed upon (i.e., subtracted from) the equation for N_X can be pictured as follows:

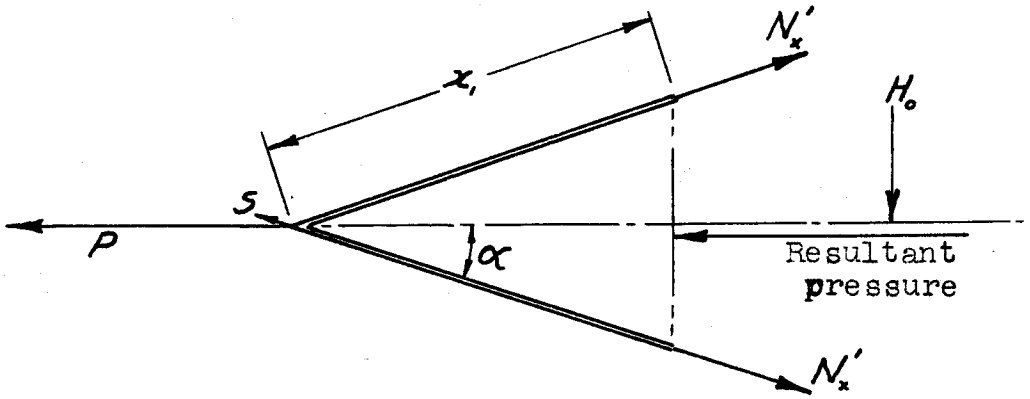

It can be seen that the "S" component is negligible and that the other component is $P = \gamma H_o \pi \cdot (x_1 \sin\alpha)^2$. Therefore, the correction to the N_X expression is:

$$N_x' = \frac{\gamma H_o \pi (x_1 \sin\alpha)^2}{2\pi (x \sin\alpha)\cos\alpha} = \left(\frac{\gamma H_o}{2} \tan\alpha\right) \frac{x_1^2}{x},$$

and the final corrected longitudinal load becomes:

$$N_x = \left(\frac{\gamma}{9\cos\alpha}\right)\left\{x^2(1-3\sin^2\alpha) - \frac{1}{x}\left(\frac{x_2^3 - x_1^3}{\ln \frac{x_2}{x_1}}\right)\left[\ln x + \frac{1}{3} - (1-3\nu)\sin^2\alpha - \left(\frac{\ln^2 x_2 - \ln^2 x_1}{2\ln \frac{x_2}{x_1}}\right)\right]\right\}\cos\varphi + \left(\frac{\gamma H_o}{2}\tan\alpha\right)\cdot \left[x - \frac{\left(\frac{1}{2} - \nu\right)}{x}\cdot\left(\frac{x_2^2 - x_1^2}{\ln \frac{x_2}{x_1}}\right) - \frac{x_1^2}{x}\right] \qquad (5')$$

The particular section and fluid under consideration here gives the following physical values for the constants in the equations:

$$\nu = 0.3 \qquad \gamma = 62.4\ \frac{lb.}{ft.^3} \qquad x_1 = 57.34\ ft.$$

$$\alpha = 5.0^\circ \qquad H_o = 600\ ft \qquad x_2 = 75.41\ ft.$$

Thus, the section to be considered looks like the following:

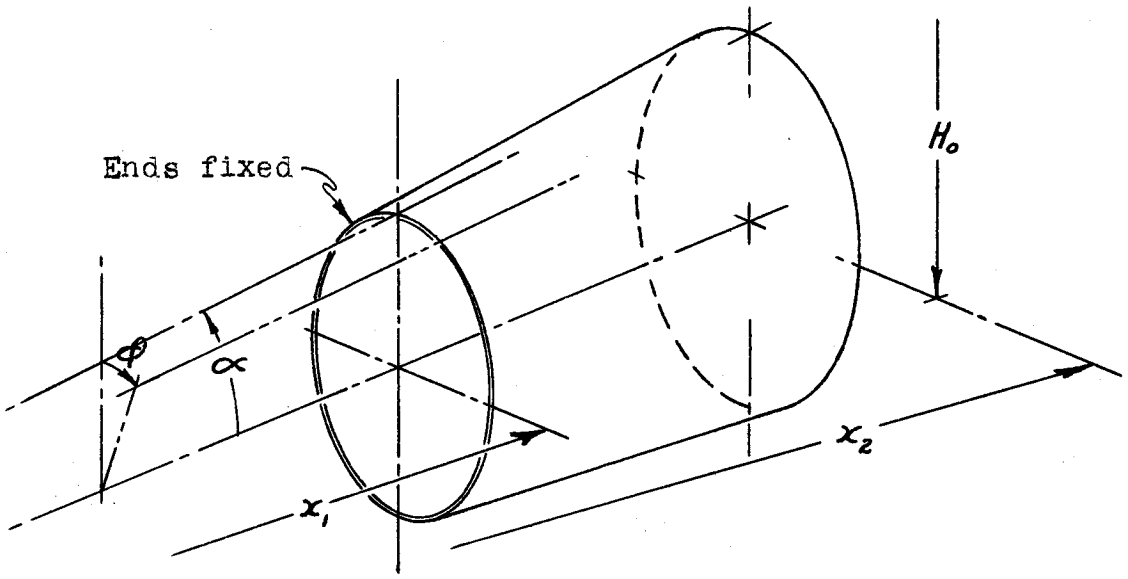

Note the origins and directions of the x and φ coordinates.

Substituting the physical constants, the final stress state equations become:

$$\begin{cases} N_\varphi = 0.0397\ \frac{lb.}{in.}\left(6881 - \frac{x}{ft.}\cos\varphi\right)\frac{x}{ft.} \\ N_{x\varphi} = 0.1517\ \frac{lb.}{in.}\left(\frac{292500\,ft.}{x} - \frac{x^2}{ft.^2}\right)\sin\varphi \\ N_x = 0.567\ \frac{lb.}{in.}\left[\frac{x^2}{ft^2} - \frac{898060\,ft.}{x}\left(\ln x - 4.0125\right)\right]\cos\varphi + \\ \qquad + 136.5\ \frac{lb.}{in.}\left(\frac{x}{ft.} - \frac{5043\,ft.}{x}\right). \end{cases}$$

The values of these running loads have been calculated along the critical elements and plotted on the following sheet. It can be verified that the values of N_φ vary directly with x and the curves extended pass through the origin. The curves of N_x have the characteristic curvatures for top and bottom of fixed-end distributed-load beams, but the effect of axial thrust is to appreciably rotate the curves. The values of N_x are typical for a beam with distributed load.

Applying the allowable tensile stress for structural grade steel to the maximum hoop tension load, the necessary thickness is found to be:

$$t = \frac{20.82 \text{ kips/in.}}{18 \text{ ksi}} = 1.157 \text{ in. (say } 1\tfrac{3}{16} \text{ in.)}.$$

Actually, an appreciable saving of material could be made by using tapered sheet so as to go from 7/8 thickness at the smaller end to 1-3/16 thickness at the larger end. Such a procedure would alter the forms of $C_1(\varphi)$ and $C_2(\varphi)$ since they are based on deflection considerations and were simplified by converting to the N's. That is, the integrals on pages 42 and 43 would have to be:

$$\int_{x_1}^{x_2} \frac{N_{x\varphi}}{x}\, dx = 0, \quad \text{and}$$

$$\int_{x_1}^{x_2} \frac{(N_x - \nu N_\varphi)}{x}\, dx = 0.$$

Since thickness would be proportional to x, that quantity has been used in place of t. The result would be to change the

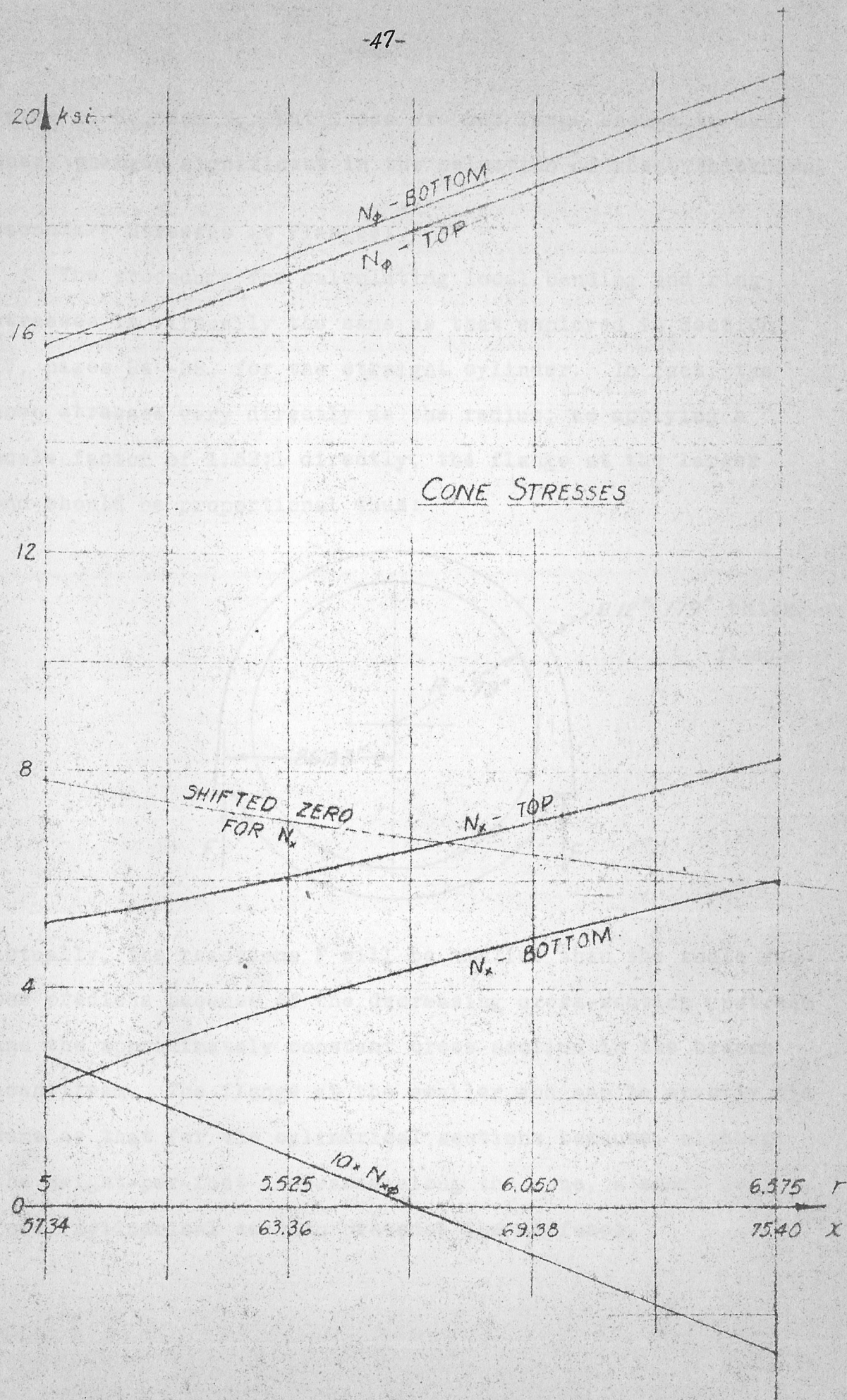
20 ksi
16
12
8
4
0
N_ϕ - BOTTOM
N_ϕ - TOP
CONE STRESSES
SHIFTED ZERO FOR N_x
N_x - TOP
N_x - BOTTOM
$10 \times N_{x\phi}$
5
5.525
6.050
6.575
r
57.34
63.36
69.38
75.40
x

forms of $N_{x\phi}$ and N_x; but these are not large enough to make their changes significant in the selection of sheet thickness.

Secondary Stresses at Flanges:

The procedure for calculating local bending and ring stresses is virtually the same as that employed in Section IV, pages 24 -28, for the straight cylinder. In fact, the hoop stresses vary directly as the radius; so applying a scale factor of 1.32:1 directly, the flange at the larger end should be proportional thus:

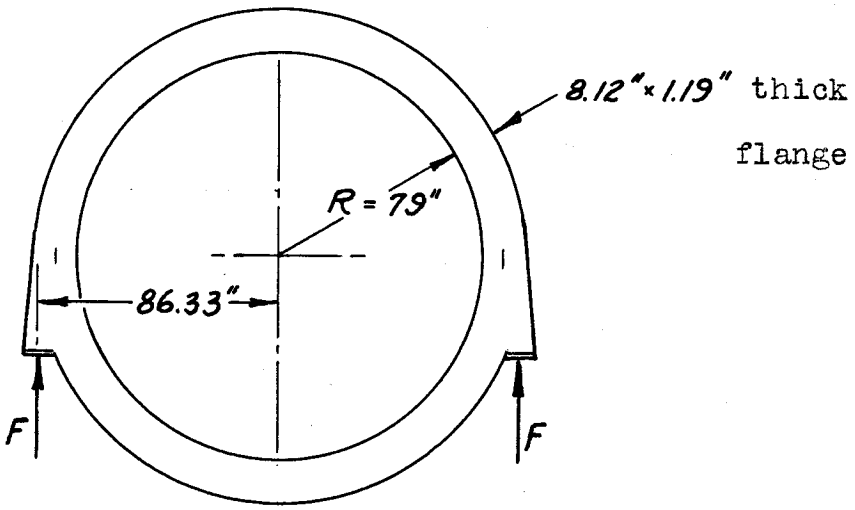

Actually, the reactions F will be smaller than the scale factor predicts because of the decreasing cross-section upstream and the approximately constant cross-section in the branch downstream. The flange at the smaller end can be exactly the same as that for the cylindrical sections because, although the weight-per-foot increases along the cone, a short (six-foot) cylindrical section precedes the diffuser.

Part-Full Condition:

The techniques of page 29 and sequence can be applied to the conical shell if the conical coordinate system of this section is used. That is, moments would have to be added to the elemental surface illustrated on page 30; and exactly the same series solutions for the displacements would be applied. In this case, ℓ would be replaced by (x_2-x_1) as far as constants are concerned.

The differential equations of equilibrium would be complicated by additional terms as were those for conical membrane theory. However, the algebraic equations for evaluating coefficients would be very little different and the work of solving them would be no more difficult. This is the particular beauty of having set up the Fourier expansion of the loading (pressure) equation.

No attempt has been made to carry through this solution because stresses would be of the same order as those found for the cylindrical section. Therefore, the negligibility of buckling considerations has been established and the shell as proportioned is assumed to be stable under all part-full loadings.

VI. DOUBLE-CURVED SECTION

As with the other two sections previously considered, the double-curved nozzle section is eighteen feet long and has virtually fixed ends. Further, the range of diameters from one end to the other is the same as that for the conical diffuser. The curvature of the element lines complicates the analysis; but some very important conclusions can be drawn from the two previous analyses.

Heavy enough sheet is required for such high design pressures that stability of the sheet under part-full conditions is not a problem. Further, the high-head hoop tensions determine the sheet thickness rather than any of the other stresses; and the N_φ equation is much the easiest to write.

Consider the following element of the double-curved surface under membrane stresses only; i.e., neglect transverse bending moments:

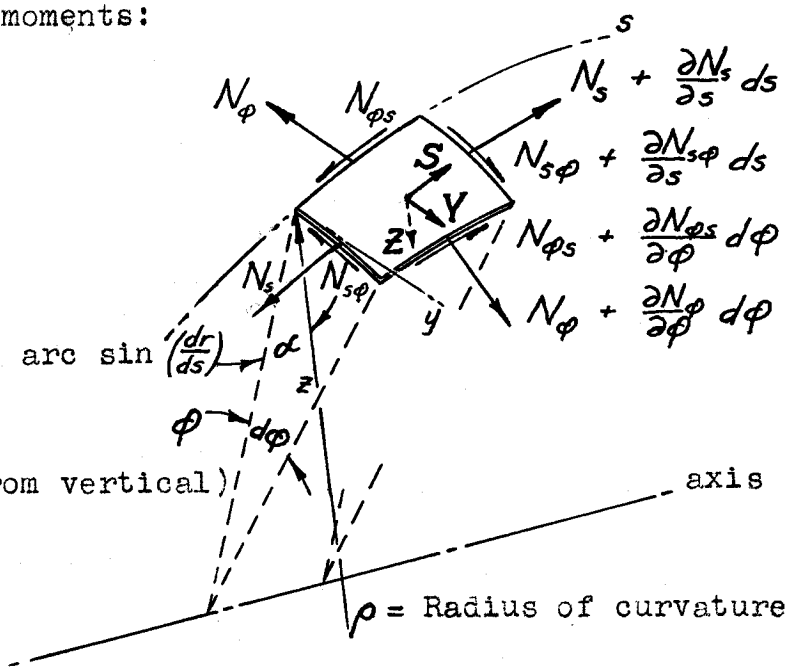

This is seen to be very much like the conical element shown on page 42; and equilibrium in the Z-direction yields the hoop tension with the additional difficulty that curvature along the elements brings the N_s loads into the equation. This same effect is to be noted in Plates and Shells[3], equation (j) on page 358, even though the different coordinate system complicates the comparison. For this case, equilibrium in the Z-direction yields:

$$(\cos\alpha)\cdot N_\phi \, ds \, d\phi + \left(\frac{1}{\rho}\right)\cdot N_s \, r \, d\phi \, ds = -Z\cdot r \, d\phi \, ds$$

$$= \gamma r \, d\phi \, ds \, (H_o - r\cos\phi).$$

Checking the trigonometry of the element orientation will show that:

$$\cos\alpha = \left[1 - \left(\frac{dr}{ds}\right)^2\right]^{\frac{1}{2}},$$

$$\frac{1}{\rho} = \left[1 - \left(\frac{dr}{ds}\right)^2\right]^2 \frac{d^2r}{ds^2}.$$

Substituting these into the equilibrium equation and simplifying, one gets:

$$N_\phi = \frac{\gamma r}{\sqrt{1-\left(\frac{dr}{ds}\right)^2}}(H_o - r\cdot\cos\phi) - r\left[1-\left(\frac{dr}{ds}\right)^2\right]^{\frac{3}{2}}\left(\frac{d^2r}{ds^2}\right)N_s \qquad (1)$$

Note the similarity between the first part of this expression and the equations for the cylindrical section (1 on p. 21) and the conical section (3 on p. 41). The maximum is likely to occur for largest radius, r, steepest slope, $\frac{dr}{ds}$, or largest

negative second derivative, $\frac{d^2r}{ds^2}$.

For this nozzle shape, slopes and curvatures are zero at the ends; and hoop tension at the bigger end is:

$$N_\varphi = 5.2 \frac{lb.}{in.\,ft.^2}\ 6.5\,ft.\,(600\,ft. + 6.5\,ft.) = 20.50 \frac{kips}{in.}$$

The steepest slope, $\frac{dr}{ds} = 0.171$, occurs at the hoop where radius, r = 6.0 ft. and curvature is zero again; so circumferential tension is:

$$N_\varphi = \frac{5.2 \frac{lb.}{in.\,ft.^2}}{\sqrt{1-.029}}\ 6.0\,ft.\,(600\,ft. + 6\,ft.) = 19.18 \frac{kips}{in.}$$

The largest negative second derivative, $\frac{d^2r}{ds^2} = -0.16$, occurs at r = 6.4 and $\frac{dr}{ds} = 0.06$; so these values give:

$$N_\varphi = \frac{5.2 \frac{lb.}{in.\,ft.^2}}{\sqrt{1-.0036}}\ 6.4\,ft.\,(600\,ft. + 6.4\,ft.) + 6.4\,ft.\,(1-.0036)^{\frac{3}{2}} \cdot$$

$$\cdot(-.16)N_s = 20.22 \frac{kips}{in.} - 1.02\,N_s$$

Obviously the last term of this expression does not contribute enough to the total for consideration, particularly since the previous studies have shown N_s to be appreciably smaller than N_φ. Therefore, the proper sheet thickness appears to be:

$$t = \frac{20.5\ kips/in.}{18\ ksi} = 1.139\ in.\ (\text{say } 1\tfrac{1}{4}\ in.).$$

This does not decrease linearly as one approaches the smaller end; so the entire nozzle should maintain this wall thickness as a minimum.

The other equations are somewhat more involved and might be too difficult of solution for purely analytical means.

However, graphical integrations may be the way to a good answer. Note that the expression for N_ϕ involves the radius, r, and the sine of the wall angle, $\frac{dr}{ds}$, as the unknowns. If these two additional variables are used, the equilibrium equations in the Y- and S-directions can be written by comparison with those for the conical section at the top of page 42:

$$\frac{\partial N_{s\phi}}{\partial s} ds(r\,d\phi) + N_{s\phi} ds\left(\frac{dr}{ds} d\phi\right) + \frac{\partial N_\phi}{\partial \phi} d\phi\, ds = -\gamma r\, d\phi\, ds = 0$$

$$\frac{\partial N_s}{\partial s} ds(r\,d\phi) + N_s ds\left(\frac{dr}{ds} d\phi\right) + \frac{\partial N_{s\phi}}{\partial \phi} d\phi\, ds - N_\phi ds\left(\frac{dr}{ds} d\phi\right)$$

$$= -S r\, d\phi\, ds = 0$$

Simplifying and substituting the value of N_ϕ from equation (1), the differential equations become:

$$r \cdot \frac{\partial N_{s\phi}}{\partial s} + \left(\frac{dr}{ds}\right) N_{s\phi} + \frac{\gamma r^2}{\sqrt{1-\left(\frac{dr}{ds}\right)^2}} \cdot \sin\phi = 0 \qquad (2)$$

$$r \cdot \frac{\partial N_s}{\partial s} + \left(\frac{dr}{ds}\right) N_s + \frac{\partial N_{s\phi}}{\partial \phi} + \frac{\gamma r}{\sqrt{\left(\frac{dr}{ds}\right)^{-2}-1}}(-H_o + r\cos\phi) = 0 \qquad (3)$$

Obviously, r is an extra variable but dependent upon the shape of the nozzle and hence upon the length along the elements, s.

First step of an analytical solution would be to express r as some function of s and to determine its derivative, $\frac{dr}{ds}$. The validity of the solution will depend upon how close to the actual nozzle shape one can approximate with some analytical function. The ease with which a solution can be obtained depends upon the simplicity of the function and its derivative. We have already shown by the cone analysis that the straight-

line approximation with its constant derivative gives "exact" differential equations which were solved quite readily. Probably a cubic, trigonometric or exponential function can be made to give a satisfactory approximation even if the integrations have to be done graphically. The lack of symmetry about the point of inflection in the Tsien nozzle curve makes it very difficult to get a particularly close fit from simple analytical expressions.

The establishment of lengths along the elements as one of the variables, s, gives in effect a curvilinear set of orthogonal coordinates which neatly define the double-curved surface. Thus it would be possible to carry out the part-full analysis, but only with considerable labor. In fact, the equilibrium equations involving the moments would be particularly difficult to write.

No further elaboration is necessary for preliminary design purposes. One can say that sheet of 1-1/4 inch thickness is required for the nozzle section. Further, the discussion of ring support design given on page 46 for the conical section can be applied directly at this point.

VII. CONCLUSIONS

The water tunnel design considered herein is structurally feasible and the analysis can be carried through to the last detail without any insurmountable difficulties. As far as this paper can go, the more involved analyses have been established and the techniques are readily applicable, not only to this problem but to numerous similar problems.

The Tsien nozzle calculations discussed in section two and developed in Appendix A neatly systematize the procedure and point the way for future investigators. The Φ's, α's and β's tabulated in the appendix will be useful to future calculators directly; and the typical calculation for the final step makes a good tabular method available.

The Fourier expansion of the half-full loading condition is most noteworthy for its usefullness in circumventing discontinuities which so often plague the analyst with extra boundary conditions and complex solutions. The Fourier expansion of loadings is particularly useful in plate and shell problems.

Membrane theory has been applied successfully to shells of revolution about a horizontal axis which are loaded by gravity and internal pressure. Shells of revolution about vertical axes are analyzed more simply under these same loadings and they have been treated in some detail by Timoshenko[3] on page 363 of Plates and Shells. Solutions of these problems are quite direct when the elements are straight lines; and simpli-

fied methods of handling surfaces with curved elements have been indicated herein. While precise analysis is possible for cylinders and cones, the accuracy (and probable difficulty) of the double-curved analysis is dependent upon the quality of the approximation to the actual surface by some simple analytical function.

Analysis which involves transverse bending of shells has been completed for one simple part-full case and the methods are extremely tedious. Further, accuracy is increased only by extension of the series solutions, all of which do not converge very rapidly. The transverse bending moment expressions are particularly bad offenders in not converging with any rapidity. However, much can be learned from this analysis in estimating the amount of labor involved in obtaining a certain degree of accuracy in this and similar solutions.

Fortunately, this design calls for significant accuracy only in the membrane theory analysis. This will be true for other problems where relatively thick sheet results from extremely high internal pressures. The involved part-full analysis served only to prove the negligibility of transverse bending and direct loads for that condition. Had they been higher, i.e. had they threatened buckling, the problem of curved sheet buckling under complicated loadings would have been raised; and that problem has not been brought to anything like a practical analytical solution.

REFERENCES

1. Tsien, Hsue-Shen, "On the Design of the Contraction Cone for a Wind Tunnel," Journal of the Aeronautical Sciences, vol. 10, no. 2, p. 68 et seq., February 1943.

2. Roark, R.J., Formulas for Stress and Strain, McGraw-Hill Book Co., Inc., New York, 1943.

3. Timoshenko, S., Theory of Plates and Shells, McGraw-Hill Book Co., Inc., New York, 1940.

4. Steel Construction, American Institute of Steel Construction, New York, 1941.

5. ANC-5 Strength of Aircraft Elements, Army-Navy-Civil Committee on Aircraft Requirements, Washington, 1944.

6. Schorer, H., "Design of Large Pipe Lines", Trans. of the Amer. Soc. C.E., vol. 98, p. 101 et seq., New York, 1933.

7. Sechler and Dunn, Airplane Structural Analysis and Design, John Wiley & Sons, Inc., New York, 1942.

8. Timoshenko, S., Theory of Elastic Stability, McGraw-Hill Book Co., Inc., New York, 1936.

A. TSIEN CALCULATIONS

Calculation of $\phi^m(x)$:

Remember that $\phi(x)$ is the probability function which is tabulated in many mathematical handbooks:

$$\Phi(x) = \frac{1}{\sqrt{2\pi}} e^{-\frac{x^2}{2}}.$$

Also given in the tables is the area under the curve as well as the second, third and fourth derivatives. The first derivative is just:

$$\Phi'(x) = \frac{-x}{\sqrt{2\pi}} e^{-\frac{x^2}{2}} = x \cdot \Phi(x).$$

Above the fourth derivative, the derivatives are evaluated by the recurrence relation:

$$\Phi^{(m)} = -\left[x \cdot \Phi^{(m-1)}(x) + (m-1) \cdot \Phi^{(m-2)}(x)\right].$$

These derivatives are basic to the Tsien calculation.

The tables which follow give values required in the calculation up the nineteenth derivative. Since the nozzle will normally lie between x = -2.5 and x = 2.5, the functions have been evaluated for every half-unit between these limits. The curves of some of these functions have been plotted on page A-5 to indicate their nature. In the tables originally used for this calculation, it was found convenient to intersperse columns for $x\phi^{(m-1)}$ and $(m-1) \cdot \phi^{(m-2)}$ between $\phi^{(m-1)}$ and $\phi^{(m)}$ columns, thus making the checking back over calculations more direct.

Values of $\int_0^x \phi(x)dx$ and $\phi^{n}(x)$:

x	* $\int_0^x \phi\, dx$	* ϕ	ϕ^{i}	* ϕ^{ii}	* ϕ^{iii}	* ϕ^{iv}	ϕ^{v}
2.5	.4938	.0175	- .0438	.0920	- .1424	.0800	.3696
2	.4772	.0540	- .1080	.1620	- .1080	- .2700	.9720
1.5	.4332	.1295	- .1942	.1619	.1457	- .7043	.4737
1	.3413	.2420	- .2420	0	.4839	- .4839	- 1.4517
0.5	.1915	.3521	- .1760	- .2641	.4841	.5501	- 2.2114
0	0	.3989	0	- .3989	0	1.1968	0
- 0.5	- .1915	.3521	.1760	- .2641	- .4841	.5501	2.2114
- 1	- .3413	.2420	.2420	0	-..4839	- .4839	1.4517
- 1.5	- .4332	.1295	.1942	.1619	- .1457	- .7043	- .4737
- 2	- .4772	.0540	.1080	.1620	.1080	- .2700	- .9720
- 2.5	- .4938	.0175	.0438	.0920	.1424	.0800	- .3696

* Taken directly from a mathematical handbook.

x	vi ϕ	vii ϕ	viii ϕ	ix ϕ	x ϕ	xi ϕ
± 2.5	- 1.3240	± 1.0949	6.5308	∓ 25.0862	3.9383	± 241.016
± 2	- .5940	∓ 4.6440	13.4460	± 10.2600	- 141.5340	± 180.468
± 1.5	2.8110	∓ 7.0584	- 9.0894	± 70.1013	- 23.3474	∓ 665.992
± 1	3.8712	± 4.8390	- 31.9374	∓ 6.7746	294.2112	∓ 226.465
± 0.5	- 1.6448	± 14.0908	4.4682	∓ 114.9605	17.2664	± 1 140.972
0	- 5.9840	0	41.8880	0	- 376.9920	0

x	xii ϕ	xiii ϕ	xiv ϕ	xv ϕ	xvi ϕ
± 2.5	- 645.861	∓ 1 277.540	11 590.04	∓ 11 089.55	- 146 126.78
± 2	1 195.938	∓ 4 557.492	- 6 432.21	± 76 669.31	249 821.77
± 1.5	1 255.809	± 6 108.190	- 25 487.80	∓ 47 282.96	453 241.47
± 1	- 3 009.858	± 5 727.438	33 400.72	∓ 113 584.85	- 387 425.89
± 0.5	- 760.416	∓ 13 311.456	16 541.14	± 178 089.82	- 337 161.95
0	4 146.912	0	- 53 909.86	0	808 647.84

x	xvii Ø	xviii Ø	xix Ø
± 2.5	± 542 750	1 127 281	∓ 12 587 697
± 2	∓ 1 726 352	- 794 265	± 32 662 874
± 1.5	± 76 665	- 7 820 103	± 10 350 182
± 1	± 2 204 784	4 381 456	∓ 44 067 560
± 0.5	∓ 2 680 856	4 391 325	± 46 059 745
0	0	- 13 747 013	0

Φ^{VIII} Φ^{VII} Φ^{VI} Φ^{V} Φ^{IV} Φ' Φ'' Φ''' Φ^{IV} Φ^{V} Φ^{VI} Φ^{VII} Φ^{VIII}

$\int_0^x \Phi\, dx$

7 6 5 4 3 2 1 0 -1 -2 -3 -4 -5 -6 -7

2 1 0 -1 -2

Φ'' CURVES

Calculation of ψ, u and v:

The equations given for ψ, u and v on pages 10 and 11 of the text can be simplified into the following forms:

$$\psi(x,r) = 0.2037 r^2 \left[1.9545 + \int_0^x \phi \, dx + \sum_{n=1}^{\infty} \alpha_n \phi^{2n-1}\right],$$

where $\alpha_n(r) = \frac{(-1)^n}{(n+1)(n!)^2} \cdot \left(\frac{r}{2}\right)^{2n} = -\frac{r^2}{4n(n+1)} \alpha_n$;

$$u(x,r) = 0.4074 \left[1.9545 + \int_0^x \phi \, dx + \sum_{n=1}^{\infty} \beta_n \phi^{2n-1}\right],$$

where $\beta_n(r) = \frac{(-1)^n}{(n!)^2} \cdot \left(\frac{r}{2}\right)^{2n} = -\frac{r^2}{4n^2} \beta_n$;

$$v(x,r) = -0.2037 r \sum_{n=0}^{\infty} \gamma_n \phi^{2n},$$

where $\gamma_n(r) = \frac{(-1)^2}{(n+1)(n!)^2} \cdot \left(\frac{r}{2}\right)^{2n} = \alpha_n(r)$.

Note particularly the recurrence relation for the coefficients of the ϕ series terms.

Especially important to this standardized procedure is the introduction of the α, β and γ coefficients which were not established in the Tsien paper. These can be used on any nozzle calculation if the flow to be investigated falls in the particular range of the radii used here. The following tables have been worked out for r = 0.8, 1.2, 1.6, 2.0, 2.4 and 2.8.

Values of $\alpha_n(r)$ and $\delta_n(r)$:

		Multiplier:	$-\frac{r^2}{24}$		$-\frac{r^2}{48}$		$-\frac{r^2}{80}$		$-\frac{r^2}{120}$	
r	r^2	$\alpha_1 = -\frac{r^2}{8}$	$\alpha_2 \cdot 10^m \downarrow$		$\alpha_3 \cdot 10^m \downarrow$		$\alpha_4 \cdot 10^m \downarrow$		$\alpha_5 \cdot 10^m \downarrow$	
0.8	0.64	- 0.080	2.133	3	- 2.844	5	2.276	7	- 1.2136	9
1.2	1.44	- 0.180	1.080	2	- 3.240	4	5.832	6	- 6.9984	8
1.6	2.56	- 0.320	3.413	2	- 1.820	3	5.825	5	- 1.2428	6
2.0	4.00	- 0.500	8.333	2	- 6.944	3	3.472	4	- 1.1574	5
2.4	5.76	- 0.720	1.728	1	- 2.074	2	1.493	3	- 7.1664	5
2.8	7.84	- 0.980	3.201	1	- 5.229	2	5.124	3	- 3.3479	4

	$-\frac{r^2}{168}$		$-\frac{r^2}{224}$		$-\frac{r^2}{288}$		$-\frac{r^2}{360}$		$-\frac{r^2}{440}$	
r	$\alpha_6 \cdot 10^m$		$\alpha_7 \cdot 10^m$		$\alpha_8 \cdot 10^m$		$\alpha_9 \cdot 10^m$		$\alpha_{10} \cdot 10^m$	
0.8	4.6234	12	- 1.3210	14	2.9355	17	- 5.2186	20	7.5907	23
1.2	5.9986	10	- 3.8563	12	1.9281	14	- 7.7125	17	2.5241	19
1.6	1.8937	8	- 2.1643	10	1.9238	12	- 1.3680	14	7.9594	17
2.0	2.7557	7	- 4.9209	9	6.8347	11	- 7.5941	13	6.9037	15
2.4	2.4570	6	- 6.3181	8	1.2636	9	- 2.0218	11	2.6467	13
2.8	1.5623	5	- 5.4682	7	1.4886	8	- 3.2417	10	5.7762	12

Values of $\beta_n(r)$:

	Multiplier:		$-\frac{r^2}{16}$		$-\frac{r^2}{36}$		$-\frac{r^2}{64}$		$-\frac{r^2}{100}$	
r	r^2	$\beta_1 = -\frac{r^2}{4}$	$\beta_2 \cdot 10^m$	$\downarrow$	$\beta_3 \cdot 10^m$	$\downarrow$	$\beta_4 \cdot 10^m$	$\downarrow$	$\beta_5 \cdot 10^m$	$\downarrow$
0.8	0.64	- 0.16	6.400	3	- 1.138	4	1.138	6	- 7.2818	9
1.2	1.44	- 0.36	3.240	2	- 1.296	3	2.916	5	- 4.1990	7
1.6	2.56	- 0.64	1.024	1	- 7.282	3	2.913	4	- 7.4565	6
2.0	4.00	- 1.00	2.500	1	- 2.778	2	1.736	3	- 6.9444	4
2.4	5.76	- 1.44	5.184	1	- 8.294	2	7.465	3	- 4.2998	4
2.8	7.84	- 1.96	9.604	1	- 2.092	1	2.562	2	- 2.0087	3

	$-\frac{r^2}{144}$		$-\frac{r^2}{196}$		$-\frac{r^2}{256}$		$-\frac{r^2}{324}$		$-\frac{r^2}{400}$	
r	$\beta_6 \cdot 10^m$		$\beta_7 \cdot 10^m$		$\beta_8 \cdot 10^m$		$\beta_9 \cdot 10^m$		$\beta_{10} \cdot 10^m$	
0.8	3.2363	11	- 1.0568	13	2.6419	16	- 5.2186	19	8.3498	22
1.2	4.1990	9	- 3.0850	11	1.7353	13	- 7.7125	16	2.7765	18
1.6	1.3256	7	- 1.7314	9	1.7314	11	- 1.3680	13	8.7554	16
2.0	1.9290	5	- 3.9368	7	6.1512	9	- 7.5941	11	7.5941	13
2.4	1.7199	5	- 5.0545	7	1.1373	8	- 2.0218	10	2.9114	12
2.8	1.0936	4	- 4.3745	6	1.3397	7	- 3.2417	9	6.3538	11

Calculation of ψ, u, v and w:

The table used for calculating the values of ψ, u, v and w at a particular point in the flow being investigated has been set up on the next page; and a typical computation has been carried out on the following page to give an idea of the rate of convergence. The point illustrated is (x,r) = (-2.0,1.2) which is plotted in the middle left-hand side of the diagram on page 12 of the text. ψ converges more rapidly than do the velocities in all cases; and frequently functions did not have to be tabulted as far as they were known for consistent accuracy.

Table for Computing ψ, u, v and w at a Point (x,r):

n	ϕ^{2n-1} & ϕ^{2n}	α_n	β_n	$\alpha_n \phi^{2n-1}$	$\beta_n \phi^{2n-1}$	$\alpha_n \phi^{2n}$
				1.9545 $\int \phi \, dx$	1.9545 $\int \phi \, dx$	ϕ
1	ϕ^{i} ϕ^{ii}	α_1	β_1	$\alpha_1 \phi^{i}$	$\beta_1 \phi^{i}$	$\alpha_1 \phi^{ii}$
2	ϕ^{iii} ϕ^{iv}	α_2	β_2	$\alpha_2 \phi^{iii}$	$\beta_2 \phi^{iii}$	$\alpha_2 \phi^{iv}$
3	ϕ^{v} ϕ^{vi}	α_3	β_3	$\alpha_3 \phi^{v}$	$\beta_3 \phi^{v}$	$\alpha_3 \phi^{vi}$
.	.	.	.	.	.	.
.	.	.	.	.	.	.
.	.	.	.	.	.	.
				$\sum$	$\sum$	$\sum$
				$.2037 \, r^2$	$.4074$	$-.2037 \, r$
		Products =		$\psi(x,r)$	$u(x,r)$	$v(x,r)$
				$w(x,r)$	$= \sqrt{u^2 + v^2}$	

Computation of ψ, u, v and w at (-2.0, 1.2):

n	ϕ^{2n-1} & $\phi^{2n} \cdot 10^m$ ↓	$\alpha_n \cdot 10^m$ ↓	$\beta_n \cdot 10^m$ ↓	$\alpha_n \phi^{2n-1} \cdot 10^m$ ↓	$\beta_n \phi^{2n-1} \cdot 10^m$ ↓	$\alpha_n \phi^{2n} \cdot 10^m$ ↓
				1.9545	1.9545	
				- .4772	- .4772	5.400 2
1	1.080 1	-1.800 1	-3.600 1	-1.944 2	-3.888 2	
	1.620 1					-2.916 2
2	1.080 1	1.080 2	3.240 2	1.166 3	3.499 3	
	-2.700 1					-2.916 3
3	-9.720 1	-3.240 4	-1.296 3	3.149 4	1.260 3	
	-5.940 1					1.925 4
4	4.644 0	5.832 6	2.916 5	2.708 5	1.354 4	
	1.345 -1					7.842 5
5	-1.026 -1	-6.998 8	-4.199 7	7.180 7	4.308 6	
	-1.415 -2					9.905 6
6	-1.805 -2	5.999 10	4.199 9	-1.083 7	-7.578 7	
	1.196 -3					7.174 7
				1.459 37	1.443 32	0.022 206
				0.293 328	0.407 40	-0.244 44
		ψ =		0.428 074	0.588 008	-0.005 428
					0.345 753 +	0.000 029
			w^2	=	0.345 782	
			w	=	0.588 03	

B. FOURIER ANALYSIS

The pressure distribution about the circumference of the half-full cylinder is zero for $0 \leq \phi < \frac{\pi}{2}$ and for $\frac{3\pi}{2} < \phi < 2$; and it can be expressed as:

$$P(\phi) = 62.4 \frac{lb.}{ft.^3} R(-\cos\phi) \qquad \text{for } \frac{\pi}{2} \leq \phi \leq \frac{3\pi}{2}.$$

Therefore, the problem to be undertaken here is the expansion of the function:

$$f(\phi) = \frac{P \ ft.^3}{R \cdot 62.4 \ lb.} = -\cos\phi \qquad \text{for } \frac{\pi}{2} \leq \phi \leq \frac{3\pi}{2}$$

and equal to zero elsewhere in the interval $0 \leq \phi < 2\pi$.

The loading condition and the curve of $f(\phi)$ have been given on page 17 of the text. The shape of this curve points out the significant terms in the general Fourier expansion:

$$f(\phi) = \sum_{n=1}^{\infty} a_n \sin n\phi + \sum_{n=0}^{\infty} b_n \cos n\phi.$$

Complete symmetry indicates that all a_n's are zero. Further, although it was not immediately apparent to the author, integration showed that all odd b_n's above b_1 are also zero.

Values of the b_n's were obtained from the well-known Fourier formulae:

$$b_o = \frac{1}{2\pi} \int_0^{2\pi} f(\phi) \, d\phi, \quad \text{and}$$

$$b_n = \frac{1}{\pi} \int_0^{2\pi} f(\phi) \cos n\phi \, d\phi.$$

These were broken down into three intervals of integration

thus:

$$b_o = \frac{1}{2\pi}\left[\int_0^{\frac{\pi}{2}} 0\cdot d\phi - \int_{\frac{\pi}{2}}^{\frac{3\pi}{2}} \cos\phi\, d\phi + \int_{\frac{3\pi}{2}}^{2\pi} 0\cdot d\phi\right]$$

$$= -\frac{1}{2\pi}\int_{\frac{\pi}{2}}^{\frac{3\pi}{2}} \cos\phi\, d\phi$$

$$b_n = -\frac{1}{\pi}\int_{\frac{\pi}{2}}^{\frac{3\pi}{2}} \cos\phi\, \cos n\phi\, d\phi.$$

The first few integrals will be evaluated here:

$$b_o = -\frac{1}{2\pi}\int_{\frac{\pi}{2}}^{\frac{3\pi}{2}} \cos\phi\, d\phi = -\frac{1}{2\pi}\left[\sin\phi\right]_{\frac{\pi}{2}}^{\frac{3\pi}{2}} =$$

$$= -\frac{1}{2\pi}\left[-1-1\right] = \frac{1}{\pi} = 0.318\,309\,9$$

$$b_1 = -\frac{1}{\pi}\int_{\frac{\pi}{2}}^{\frac{3\pi}{2}} \cos^2\phi\, d\phi = -\frac{1}{2\pi}\left[\phi + \cancel{\frac{1}{2}\sin 2\phi}\right]_{\frac{\pi}{2}}^{\frac{3\pi}{2}} =$$

$$= -\frac{1}{2\pi}\left[\frac{3\pi}{2} - \frac{\pi}{2}\right] = -\frac{1}{2} = -0.500$$

$$b_2 = -\frac{1}{\pi}\int_{\frac{\pi}{2}}^{\frac{3\pi}{2}} \cos\phi\, \cos 2\phi\, d\phi = \frac{1}{\pi}\int_{\frac{\pi}{2}}^{\frac{3\pi}{2}} (\cos\phi - 2\cos^3\phi)\, d\phi$$

$$= \frac{1}{\pi}\left[\cancel{\sin\phi} - \cancel{2\sin\phi} - \frac{2}{3}\sin^3\phi\right]_{\frac{\pi}{2}}^{\frac{3\pi}{2}} = \frac{1}{\pi}\left[1+1-\frac{2}{3}-\frac{2}{3}\right]$$

$$= \frac{2}{3\pi} = 0.212\,206\,6$$

The result of combining the three curves thus given have been plotted on page 17 of the text to show how the series converges on the required curve. The process can be continued readily as far as expansions of cos nØ are given in the handbooks along with integrals of powers of cos Ø.

For higher values of n, the cosine product can be expressed in the following manner:

$$\cos\phi\cos n\phi = 2^{n-1}\cos^{n+1}\phi - \frac{n}{1!}2^{n-3}\cos^{n-1}\phi +$$

$$\frac{n(n-3)}{2!}2^{n-5}\cos^{n-3}\phi - \frac{n(n-4)(n-5)}{3!}2^{n-7}\cos^{n-5}\phi +$$

$$\frac{n(n-5)(n-6)(n-7)}{4!}2^{n-9}\cos^{n-7}\phi - \text{---}$$

--- until the coefficient = 0.

It will be noted that, since even values of n are to be considered, all of the powers of cos Ø are odd. Therefore, the integrals become:

$$\int_{\frac{\pi}{2}}^{\frac{3\pi}{2}}\cos^{m}\phi\,d\phi = \int_{\frac{\pi}{2}}^{\frac{3\pi}{2}}(1-\sin^2\phi)^{\frac{m-1}{2}}(\cos\phi\,d\phi) =$$

$$= \int_{1}^{-1}(1-z^2)^{\frac{m-1}{2}}dz\ ;$$

and these are readily evaluated after the power has been expanded long-hand or by means of binomial coefficients. This procedure was continued up to m = 15 for solutions of b_n up to b_{14}.

The results have been tabulated on page 17 of the text; and the circled points plotted on the curve are the result of calculations summing the first eight terms. The approximation is seen to be very good.

C. EQUATION SOLUTIONS

The infinity of simultaneous equations (1), (2) and (3) on pages 32 and 33 of the text are solved here in groups of three by evaluating the constant coefficients according to regular algebraic procedures. First step is to select a particular value of n and equate the coefficients of sin $n\phi$ or cos $n\phi$ on the two sides of each equation. It can be seen that the left sides still involve infinite series of sin $\frac{m\pi x}{\ell}$ and cos $\frac{m\pi x}{\ell}$ while the right sides are just constants. The next step is to expand the constants as the long-established series:

$$k = \frac{4k}{\pi} \sum_{m=1,3,5,\cdots}^{\infty} \frac{\sin m\theta}{m} \quad \text{where} \quad \theta = \frac{x}{\ell}$$

is exactly what is needed in this solution. The subsequent evaluation of coefficients is from simple algebraic equations.

The form of the original equations on pages 32 and 33 shows that only even values of $\frac{m\pi x}{\ell}$ can yield results for A_{mn}; but all such terms when collected have zeros on the right-hand sides and can yield only $A_{mn} = 0$. Therefore, three equations with only two unknowns result; and one of these equations must be discounted if conflicting results are to be avoided. Since $A_{mn} = u = 0$ represents a distribution of constraints in the X-direction, it is obvious that the summation of forces in that direction (which neglected these constraints) is incorrect and that the resulting equation (1) is incomplete and must be disregarded for the remaining calculations.

The equations solved and the actual numerical results are presented here. The numerical results are to be found in one tabular collection on page 34 of the text.

For n = 0:

(2) yields nothing.

$$(3)\quad -\sum (97\,276 + m^4) C_{mo} \sin \frac{m\pi x}{\ell} = 0.555\,214 \text{ ft.}$$

$$= 0.706\,92 \text{ ft.} \sum_{m=1,3,5\cdots}^{\infty} \frac{1}{m} \sin \frac{m\pi x}{\ell}.$$

From which,

$$B_{mo} = 0 \; ; \quad C_{mo} = \frac{-0.706\,92 \text{ ft.}}{m(97\,276 + m^4)}$$

Results:

m	$C_{mo} \cdot 10^9$ in feet
1	- 7 260
3	- 2 420
5	- 1 444
7	- 1 013
9	- 764
11	- 527
13	- 432
15	- 319
17	- 230
19	- 163
21	- 115
23	- 82
25	- 58

For n = 1:

$$(2)\quad \sum [19\,744.4(3.751\,64 + m^2) B_{m1} - (74\,107 + m^2) C_{m1}] \sin \frac{m\pi x}{\ell}$$

$$= 0.152\,00 \text{ ft.} = 0.193\,532 \text{ ft.} \sum_{m=1,3,5,\cdots}^{\infty} \frac{1}{m} \sin \frac{m\pi x}{\ell}$$

$$(3)\quad \sum [2.2315(43\,592 + m^2) B_{m1} - (97\,278 + 2.6255\, m^2 + m^4) C_{m1}].$$

$$\cdot \sin \frac{m\pi x}{\ell} = -1.07174 = -1.36452 \text{ ft.} \sum_{m=1,3,5\cdots}^{\infty} \frac{1}{m} \sin \frac{m\pi x}{\ell}$$

Results:

m	$B_{m1} \cdot 10^9$	$C_{m1} \cdot 10^9$ in feet
1	62 546	76 570
3	2 311	6 979
5	496	3 279
7	178	2 127
9	81	1 533
11	42	1 141
13	23	849
15		621
17		442
19		314
21		222
23		157
25		112
27		80
29		58

For n = 2:

$$(2) \quad \sum \left[9872.2(m^2 + 15.0036) B_{m2} - (m^2 + 74{,}205.3) C_{m2} \right] \cdot \sin \frac{m\pi x}{\ell} = 0$$

$$(3) \quad \sum \left[4.4630(m^2 + 43595) B_{m2} - (m^4 + 10.502 m^2 + 97304) C_{m2} \right] \cdot \sin \frac{m\pi x}{\ell} = 0.370146 \text{ ft.} = 0.471285 \text{ ft} \sum_{m=1,3,5,\cdots}^{\infty} \frac{1}{m} \sin \frac{m\pi x}{\ell}$$

Results:

m	$B_{m2} \cdot 10^9$	$C_{m2} \cdot 10^9$ in feet
1	- 37 336	- 79 491
3	- 1 347	- 4 300
5	- 288	- 1 530
7	- 101	- 871
9	- 46	- 585
11	- 23	- 418
13		- 303
15		- 218
17		- 155
19		- 109
21		- 77
23		- 54

For n = 4:

$$(2)\quad \sum\left[4936.1(60.014+m^2)B_{m4} - (74\,599.2+m^2)C_{m4}\right]\cdot \sin\frac{m\pi x}{\ell} = 0$$

$$(3)\quad \sum\left[8.926(43604.4+m^2)B_{m4} - (977193+42.008m^2+m^4)C_{m4}\right]\cdot \sin\frac{m\pi x}{\ell} = -0.074\,027\text{ft.} = -0.094\,254\text{ft.}\sum_{m=1,3,5\cdots}^{\infty}\frac{1}{m}\sin\frac{m\pi x}{\ell}$$

Results:

m	$B_{m4}\cdot 10^9$	$C_{m4}\cdot 10^9$ in feet
1	17 268	69 715
3	533	2 432
5	111	625
7	39	280
9	17	159
11		101
13		67
15		46

For n = 6:

$$(2)\quad \sum\left[3290.7(135.032+m^2)B_{m6} - (75\,255.4+m^2)C_{m6}\right]\cdot \sin\frac{m\pi x}{\ell} = 0$$

$$(3)\quad \sum\left[13.389(43620+m^2)B_{m6} - (99511.9+94.518m^2+m^4)C_{m6}\right]\cdot \sin\frac{m\pi x}{\ell} = 0.031,722\text{ft.} = 0.040\,390\text{ft}\sum_{m=1,3,5\cdots}^{\infty}\frac{1}{m}\sin\frac{m\pi x}{\ell}$$

Results:

m	$B_{m6}\cdot 10^9$	$C_{m6}\cdot 10^9$ in feet
1	- 4 779	- 28 428
3	- 278	- 1 752
5	- 61	- 426
7	- 21	- 171
9		- 87
11		- 50

For n = 8:

$$(2)\quad \sum\left[2468.05(240.06+m^2)B_{m8}-(76\,174.2+m^2)C_{m8}\right]\cdot \sin\frac{m\pi x}{\ell}=0$$

$$(3)\quad \sum\left[17.852(43641.4+m^2)B_{m8}-(104\,338+168.032m^2+m^4)C_{m8}\right]\cdot \sin\frac{m\pi x}{\ell}=-0.017626\text{ft.}=-0.022442\text{ ft.}\sum_{m=1,3,5\cdots}^{\infty}\frac{1}{m}\sin\frac{m\pi x}{\ell}$$

Results:

m	$B_{m8}\cdot 10^9$	$C_{m8}\cdot 10^9$ in feet
1	605	4 721
3	99	798
5	34	296
7		101
9		50

For n = 10:

$$(2)\quad \sum\left[1974.44(375.09+m^2)B_{m10}-(77355.6+m^2)C_{m10}\right]\cdot \sin\frac{m\pi x}{\ell}=0$$

$$(3)\quad \sum\left[22.315(43669.2+m^2)B_{m10}-(114\,515+262.55m^2+m^4)C_{m10}\right]\cdot \sin\frac{m\pi x}{\ell}=0.011216\text{ft.}=0.014281\text{ft.}\sum_{m=1,3,5\cdots}^{\infty}\frac{1}{m}\sin\frac{m\pi x}{\ell}$$

Results:

m	$B_{m10}\cdot 10^9$	$C_{m10}\cdot 10^9$ in feet
1	- 112	- 1 077
3	- 28	- 271
5		- 109
7		- 52

For n = 12:

$$(2)\quad \sum\left[1645.37(540.13+m^2)B_{m12} - (78\,799.4+m^2)C_{m12}\right]\cdot \sin\frac{m\pi x}{\ell} = 0$$

$$(3)\quad \sum\left[26.778(43\,703.2+m^2)B_{m12} - (133\,021+378.07m^2+m^4)C_{m12}\right]\cdot \sin\frac{m\pi x}{\ell} = -0.007\,763\text{ft.} = -0.009\,884\text{ft.}\sum_{m=1,3,5,\cdots}^{\infty}\frac{1}{m}\sin\frac{m\pi x}{\ell}$$

Results:

m	$B_{m12}\cdot 10^9$	$C_{m12}\cdot 10^9$ in feet
1	12	331
3		96
5		45